Title

Techno-economic assessment of renewable methanol from biomass gasification and PEM electrolysis for decarbonization of the maritime sector in California

Authors

de Fournas, Nicolas
Wei, Max

Publication Date

2022-04-01

DOI

10.1016/j.enconman.2022.115440

Peer reviewed

Energy Conversion and Management 257 (2022) 115440

Contents lists available at ScienceDirect

Energy Conversion and Management

journal homepage: www.elsevier.com/locate/enconman

Techno-economic assessment of renewable methanol from biomass gasification and PEM electrolysis for decarbonization of the maritime sector in California

Nicolas de Fournas [1], Max Wei [*]

Energy Analysis and Environmental Impacts Department, Environmental Energy Technologies Division, Lawrence Berkeley National Laboratory, One Cyclotron Road MS 90R-2002, Berkeley, CA 94720-8136, USA

ARTICLE INFO

Keywords:
Biomass
Renewable methanol
Hydrogen
Shipping fuel
Carbon-negative
Carbon capture

ABSTRACT

At scale, biomass-based fuels are seen as long-term alternatives to conventional shipping fuels to reduce greenhouse gas emissions in the maritime sector. While the operational benefits of renewable methanol as a marine fuel are well-known, its cost and environmental performance depend largely on production method and geographic context. In this study, a techno-economic and environmental assessment of renewable methanol produced by gasification of forestry residues is performed. Two biorefinery systems are modeled thermodynamically for the first time, integrating several design changes to extend past work: (1) methanol synthesized by gasification of torrefied biomass while removing and storing underground a fraction of the carbon initially contained in it, and (2) integration of a polymer electrolyte membrane (PEM) electrolyzer for increased carbon efficiency via hydrogen injection into the methanol synthesis process. The chosen use case is set in California, with forest residue biomass as the feedstock and the ports of Los Angeles and Long Beach as the shipping fuel demand point. Methanol produced by both systems achieves substantial lifecycle greenhouse gas emissions savings compared to traditional shipping fuels, ranging from 38 to 165%, from biomass roadside to methanol combustion. Renewable methanol can be carbon-negative if the CO_2 captured during the biomass conversion process is sequestered underground with net greenhouse gas emissions along the lifecycle amounting to −57 gCO_2eq/MJ. While the produced methanol in both pathways is still more expensive than conventional fossil fuels, the introduction of CO_2eq abatement incentives available in the U.S. and California could bring down minimum fuel selling prices substantially. The produced methanol can be competitive with fossil shipping fuels at credit amounts ranging from \$150 to \$300/tCO_2eq, depending on the eligible credits.

1. Introduction

1.1. Motivation

1.1.1. The need for shipping industry decarbonization

The shipping sector represented 12% of the global transport sector energy consumption in 2016, around 300 million tons of oil equivalent. It accounts for 3% of total global greenhouse gas (GHG) emissions [1]. Maritime emissions are expected to rise significantly in the next decades with increasing international trade and maritime shipping [2] and due to slower carbon intensity reductions in shipping fuels, in the order of only 1–2% after 2015 [3]. GHG emissions growth is projected to range from 50% to 250% by 2050 under various "business-as-usual" scenarios modeled [3–5], if more stringent policies and mitigation measures are not adopted. Currently, most marine transportation uses fossil fuels such as heavy fuel oil (HFO) and marine gasoil (MGO). Besides greenhouse

Abbreviations: **AGR**, Acid gas removal; **ASU**, Air separation unit; **CCS**, CO_2 capture and storage; **EFG**, Entrained flow gasifier; **GHG**, Greenhouse gases; **HFO**, Heavy fuel oil; **HHV**, Higher heating value; **HSFO**, High sulfur fuel oil; **HVO**, Hydrotreated vegetable oil; **LCFS**, Low carbon fuel standard; **LCOP**, Levelized cost of production; **LHV**, Lower heating value; **LNG**, Liquefied natural gas; **MFSP**, Minimum fuel selling price; **MGO**, Marine gasoil; **NPV**, Net present value; **ODMT**, Oven dry metric ton; **PEM**, Polymer electrolyte membrane; **PM**, Particulate matter; **S1**, System 1; **S2**, System 2; **TRL**, Technology readiness level; **VLSFO**, Very low sulfur fuel oil; **WGS**, Water-gas shift.

* Corresponding author.
E-mail address: mwei@lbl.gov (M. Wei).
[1] Permanent institution: ETH Zürich, Rämistrasse 101, 8092 Zürich, Switzerland.

https://doi.org/10.1016/j.enconman.2022.115440
Received 4 December 2021; Received in revised form 7 February 2022; Accepted 23 February 2022
Available online 4 March 2022

gas emissions, these fuels are the significant global contributors to SOx, NOx and PM emissions, the latter being most impactful in port cities. According to the International Maritime Organization (IMO), international shipping is responsible for respectively 12% and 13% of global SOx and NOx emissions annually.

1.1.2. Recent regulations push for sustainable solutions

To address air pollution, the IMO and other governing institutions have enacted regulations that require decreasing emissions of SOx and NOx from ships. For instance, in 2015, fuel sulfur was limited to 0.1% m/m (mass by mass) in Emission Control Areas (ECA), which include coastal regions of Northern Europe and the U.S., and to 0.5% outside ECAs in 2020. In addition, the California Air Resources Board (CARB) has introduced shipping fuel regulations within 24 nautical miles of the California coastline. Current fossil alternatives compliant to the most stringent ECA limits, such as very low sulfur fuel oil or MGO, are however costly to produce, and still emit large amounts of SOx, NOx and PM into the atmosphere [6]. Besides, IMO has set ambitious goals to reduce the carbon footprint of shipping. IMO targets, relative to 2008, are to reduce GHG emissions from international shipping by 50% in 2050 and to reduce carbon intensity (CO_2 per ton-mile) by 40% for new ships by 2030 and 70% by 2050 [2,3]. Although its short- and mid-term strategies focus on speed reduction, low-carbon fuels, carbon pricing and energy efficiency measures, its long-term plan involves carbon neutral fuels.

1.1.3. Options for shipping decarbonization

Proposed alternatives to reduce the shipping industry's carbon footprint include transitioning to novel fuels or propulsion technologies including nuclear propulsion, fuel cells, batteries, liquefied natural gas (LNG), ammonia and various biofuels [4]. Each approach has its advantages and drawbacks. Biofuel development could suffer from competition with road, aviation and petrochemical sectors. However, their use would contribute much more to GHG emissions reductions than alternatives, while being compatible with current shipping infrastructure [2].

Mukherjee et al. [4] found bio-methanol to be the most promising biofuel among other options for the marine sector, based on cost, potential availability, present technology status, GHG mitigation potential, infrastructure compatibility and CO_2 capture and storage (CCS) compatibility. According to a recent S&P report [7], "in the years to come LNG, methanol, hydrogen and ammonia are all in the mix as potential alternatives marine fuels". Methanol is sulfur-free and produces very little PM and NOx when combusted. When produced from renewable sources such as biomass, captured CO_2 or decarbonized electricity, it can additionally provide significant GHG emissions reductions compared to fossil fuels. By comparison, LNG is cost-competitive in the near-term, also provides SOx and PM benefits over baseline fossil fuels but has a limited decarbonization potential. Most importantly, it does not meet long-term IMO GHG targets with only a 2% lower global warming potential than HFO [2] over its lifecycle and emitting eight times more methane emissions along its lifecycle than HFO.

A significant push in favor of methanol compared to alternatives occurred in November 2020 when the IMO approved interim guidelines for the safety of ships using methanol and ethanol, recognizing them as low carbon marine fuels. Subsequently, the first Bunkering[2] Technical Reference for Methanol was published recently by Lloyd's Register [8]. Interest in methanol as a marine fuel is growing globally and it is being used in several demonstration projects and commercial activities, mainly in Europe and Asia. Currently, 38 large methanol-powered ships are operating or on order according to DNV's online insights platform [9]. Recently, Maersk, DSV Panalpina, DFDS, SAS and Ørsted formed a partnership in 2020 to develop an industrial-scale sustainable fuel production facility in Copenhagen, aiming to deliver 250,000 tonnes of sustainable fuel including renewable methanol for Maersk ships [10]. Maersk recently announced ordering eight methanol- powered container ships, built by Hyundai Heavy Industries for 2024, and the launch of a carbon neutral ship in 2023 that will run on renewable methanol [11].

Methanol is already a commodity available worldwide, with considerable infrastructure for distribution and storage capacity in place [6]. While liquid LNG requires insulation to maintain very cold temperatures, methanol is liquid at ambient conditions, thus allowing the use of conventional fuel transport, storage, and bunkering infrastructure with small and inexpensive modifications. Out of the largest 100 international ports, 88 already have the bunkering infrastructure in place for methanol [12], and existing ships can easily be converted to use it at moderate costs [13].

1.1.4. Barriers to transitioning to low-GHG methanol

Despite its clear environmental and operational benefits compared to alternatives, some important barriers to the adoption of renewable methanol as a shipping fuel still limit its development. First, existing marine fuels such as HFO and MGO remain very inexpensive compared to more sustainable alternatives. The shipping sector additionally faces important financial challenges due to COVID-19, and the high capital costs already invested for LNG bunkering infrastructure may discourage future investment in other technologies [7]. Finally, while in other transportation sub-sectors some countries can independently implement national sustainable fuel policies, these can be much slower and more complex to coordinate in the international maritime industry.

1.2. Study focus

1.2.1. Renewable methanol production methods

Today, the vast majority of methanol worldwide is derived from natural gas reformation or coal gasification, mainly for economic reasons. Only 0.2% is produced by renewable sources [6]. To reduce the carbon intensity of methanol production, some low-carbon methanol processes have been developed. Options to decarbonize natural gas-based methanol include the injection of CO_2 from industrial sources (power plants, oil refineries, cement plants, iron and steel plants) into the methanol synthesis process, or natural gas reforming using electrical heating from renewable power.

The two main routes to further reduce the carbon footprint of methanol are (1) its production from biomass, and (2) production from a combination of hydrogen produced with renewable electricity and carbon dioxide. For the former, methanol can be produced from biomass or waste gasification, biogas upgrading and reforming or as a by-product of wood pulping. For the latter, methanol is produced through a Power-to-X process by catalytic methanol synthesis, for which the CO_2 feedstock is obtained from industrial sources, direct air capture or bioenergy with carbon capture and storage (BECCS). The produced renewable methanol is then chemically identical to fossil methanol.

In a typical biomass gasification process, a water–gas shift (WGS) unit is used downstream of the gasifier to obtain a syngas suitable for methanol synthesis. The excess carbon dioxide is commonly vented, subsequently affecting the carbon conversion of the overall process as large amounts of carbon initially contained in the feedstock are lost rather than converted to methanol. When oxygen-blown, for a higher output syngas quality, the gasification requires a source of oxygen, typically supplied by an air separation unit (ASU). This process is well-known (technology readiness levels (TRL) 8–9 [6]), as it is similar to commercial coal gasification.

An interesting hybrid technique to increase the fraction of carbon converted to methanol is to combine biomass gasification with water electrolysis by injecting the produced hydrogen into the syngas before methanol synthesis. Adding hydrogen eliminates the use of the WGS unit and the subsequent removal of excess CO_2. The oxygen produced by the

[2] The fueling of ships with marine fuels

electrolysis can furthermore replace the need for an ASU, necessary for oxygen-blown gasification. For the same unit energy of biomass, twice the quantity of methanol can be theoretically produced, and carbon conversion ratios are close to 100%.

1.2.2. Literature review

Tock et al. [14] performed a thorough techno-economic assessment of several liquid fuels production from lignocellulosic biomass, including methanol. Andersson et al. [15] assessed the techno-economics of introducing gasification-based biomass-to-methanol production into an existing chemical pulp and paper mill. Conti [16] applied a mixed-integer linear programming (MILP) optimization model for the methanol production from sawmill residue gasification to minimize supply chain overall costs in Sweden. In a series of studies, Clausen et al. [17–19] performed detailed thermodynamic modeling of similar processes, integrating some design changes compared to state of the art regarding gasification, CO_2 capture, and feedstock pre-treatment. Liu et al. [20] performed a comprehensive life cycle analysis of the environmental impacts of biomass-to-methanol production processes, and Yadav et al. [21] assessed the environmental impacts of a novel biomass gasification process including biomass alkali impregnation and other methanol synthesis design modifications.

The novel hybrid methanol production method, introduced above, is already used in four demonstration projects today: three Enerkem projects (Quebec, Rotterdam, Saragossa) and the LowLands methanol project (the Netherlands) [6]. Clausen et al. [22] techno-economically assessed this process configuration considering wood-chip feedstock, alkaline electrolysis for hydrogen production and the capture of CO_2, without modeling CO_2 transport or storage. Larose et al. [23] simulated biomass gasification with hydrogen injection from solid oxide electrolysis to demonstrate higher efficiency and carbon conversion, and Zhang et al. [24] and Butera et al. [25] each performed detailed techno-economic assessments of similar processes with various system configurations.

1.2.3. Methanol production with integrated torrefaction and optional PEM electrolysis

The present work is unique and adds to past studies in a number of important ways: by providing key system configuration changes and design extensions such as CO_2 capture and storage and H_2 from PEM electrolysis; by providing the first analysis of renewable methanol for the shipping industry in California, and by providing the first detailed economic analysis of renewable methanol competitiveness including federal and state policy incentives.

In the first modeled system, renewable methanol production with integrated torrefaction and the underground storage of captured CO_2 is modeled techno-economically for the first time. In the second modeled system, a PEM electrolyzer to supply H_2 and O_2 for methanol production with integrated torrefaction is modeled for the first time. Compared to an alkaline electrolyzer [19], the PEM technology is more responsive to typical fluctuations associated with variable renewable energy generation, an important factor when the system is powered by a supply of intermittent renewable electricity such as solar or wind. Moreover, PEM-based electrolysis equipment is expected in the long-term to have greater electrical efficiency and lower investment costs than alkaline electrolyzers [26]. In addition, economic profitability analysis of the two systems will be presented for the first time, extending the literature beyond existing studies [14,16,18,19,24,25].

The choice of California as the location of the study adds to state-of-the-art research since the large majority of techno-economic studies assessing the production of renewable methanol are located in Nordic European countries [16–19,22,25,27–29]. Few studies explore the potential of methanol produced from forest residues as a sustainable maritime fuel [2,30–32]. There is in addition very little research on biomass-to-methanol routes in the U.S. [33–35], and in many past work the syngas produced by the gasification of biomass is assumed to be converted to other end-products: biofuels (Fischer–Tropsch diesel, dimethyl ether (DME)), hydrogen, gasoline or electricity [36–39]. This study is thus the first techno-economic and environmental assessment of renewable methanol production from forest residue gasification located in California.

The choice of California is motivated by several factors. First, California is a world leader when it comes to fuel and climate policies. Tradable, performance-based CO_2eq abatement credits such as the California Low Carbon Fuel Standard (LCFS) [40] along with the recently expanded federal tax credit for CO_2 sequestration (Internal Revenue Code Section 45Q [41]) could encourage the implementation of a sustainable methanol production process by lowering production costs. Second, California's main ports, Long Beach and Los Angeles (together constituting the San Pedro Bay Port Complex), are among the busiest in the United States and worldwide, representing together respectively 31% and 74% of the national and West Coast market shares, and ranking 9th worldwide [42]. They thus represent an important demand for more sustainable marine fuels and also have existing bulk storage for liquid fuels, suitable for the storage of methanol [43]. Third, California forests represent an important source of biomass, particularly when focusing on forest residue valorization for forest management and wildfire prevention. Millions of acres of forest ecosystems in California are at significant risk of catastrophic forest fire due to recurrent drought conditions and increased climate-change induced warming. Considering recent initiatives such as California law SB 901 or California's Forest Carbon Plan, the valorization of forest residues based on their use as a biofuel feedstock can represent an important offset of costs associated with wildfire prevention and forest management.

Section 2 describes the methodology, sources of data and assumptions used to (i) assess the biomass quantities available as feedstock, (ii) model both biorefineries thermodynamically and (iii) perform the economic and environmental assessment of both systems' supply chains, for two plant locations. Section 3 subsequently presents modeled results and sensitivity analysis. These are discussed in Section 4, along with some of this study's limitations and suggestions for future research. Finally, Section 5 concludes by summarizing the key findings of this work.

2. Methodology

The main methodology is presented hereafter. More details on the modeling methods, calculations and intermediate results, as well as a more exhaustive list of assumptions for all systems and scenarios assessed are given in the Supplementary file.

2.1. Biomass supply assumptions

The forest residue biomass estimates reported in Baker et al. [36] based on Sanchez and Cabiyo [44,45] were chosen for biomass feedstock supply due to their inclusion of forestry residue sources such as logging slash and forest thinnings, their consistency with recent public policy objectives, and the spatial resolution of their estimates. In contrast to other studies (Williams et al. [46], Mitchell et al. [47] or the Billion-Ton Study [44]), the adopted supply estimates are derived after simulating active forest management practices (particularly mechanical thinning) which are consistent with recent public policy objectives, such as the Forest Carbon Plan [48]. The supply estimates represent all economically available biomass from fire- and carbon-beneficial forest management in California, which aligns very well with this study's context and motivation. The spatial scope of the data from Baker et al. [36] is also well-suited to this study with biomass quantities estimated at a county-level. This spatial resolution enhances the precision of estimating biomass transportation costs and environmental footprint.

2.1.1. Biomass type

Residues from commercial forestry operations and treatments performed for the purpose of forest restoration are the primary supply

category included in this study, corresponding to "forest management" from Baker et al. This amounts to 15.1 million dry tons in California. Their collection and chipping cost is also taken from the same study and corresponds to the average collection costs observed for 35 active forest treatment and fire treatment projects led by CAL FIRE [49]. Sawmill residues are chosen to be excluded since nearly all mill residues in California are currently already used in bioenergy production or other products [47,50,51]. Shrub and chaparral residues are also excluded due to their high collection costs [36], and limited data on their thermochemical characteristics. To determine more precisely this study's biomass thermochemical properties, the identification of the mix of forest species is necessary. The method used yielded weighted average proportions of primary forest species: a mix of Douglas-Fir, Sierran Mixed Conifer, Montane Hardwood, and Redwood species. These proportions are used to estimate precise biomass feedstock characteristics, presented in Section 3.1.2.

2.1.2. Biomass chipping

Forest residues are chipped at the roadside after their collection. As the biorefinery designed in this work integrates biomass torrefaction and milling within the plant, it can be fed with wood chips directly, and roadside grinding is assumed to be not required. The environmental impact of biomass collection and chipping is determined from the GREET model [52], and will be used further in the study. While the environmental impact of typical biomass production would account for the use of fertilizers or any indirect land use-change, the feedstock of interest here is not subject to these two factors. Thus, they are excluded from the environmental assessment boundaries.

2.1.3. Biomass storage

Biomass storage was included to assume continuous biorefinery operations. The storage facility for this study is assumed to be located at the forest biomass collection point. Based on the work done in Sahoo et al. [53], outdoor-tarped storage of wood chips was chosen for this study among other alternatives due to its combination of low energy usage (37 MJ/ODMT due to handling), low environmental impact (2.7 $kgCO_2eq$/ODMT), negligible infrastructure cost, low overall storage cost ($8.21/ODMT) and ability to decrease biomass moisture while avoiding additional moisture due to rainfall. GHG emissions during biomass storage are adopted from Sahoo et al. [53]. They include emissions resulting from fuel or power used during handling in the storage facility. Fugitive gas emissions (methane and nitrous oxide) were excluded due to limited experimental data and the complexity of their calculation.

2.1.4. Biomass transportation

Wood chips are transported to the biorefinery for conversion, by truck or rail. As rail is not always available near the roadside collection point, the forest residues are assumed to be trucked from the source to a nearby rail station in the case of rail transportation, following the methodology of Baker et al. For total distances under 45 miles, truck is preferable to rail combined with local trucking, in terms of costs and environmental impact. The definitive choice of transportation mode will thus depend on the distance from the biomass collection point to the biorefinery location, and is discussed in Section 2.3.2. Transportation costs are taken from Baker et al. [36]: $0.16 per ton-mile for truck, and $0.071 per ton-mile for rail transport. GHG emissions from biomass transportation, including fuel production and combustion, were retrieved for truck and rail options from the GREET model.

2.2. Modeling of biorefineries

2.2.1. Systems considered

A simplified layout of the first system S1 is illustrated in Fig. 1, while a more detailed design can be found in the supplementary material. Wood chips are first fed into a steam drier to lower their moisture content. After pressurization using lock hoppers, the biomass is torrefied at 300 °C, resulting in an increased heating value and modified chemical composition. After being milled, the torrefied solid is fed to an oxygen-blown entrained flow gasifier (EFG). The O_2 needed for the biomass gasification is supplied by an ASU. The high temperature syngas obtained from gasification is then chemically quenched using the torrefaction volatile gases, which decompose into H_2O, H_2, CO_2 and CO at high temperatures and increase the process efficiency. After being cooled down, the upgraded syngas, mainly composed of hydrogen and carbon monoxide, flows into a WGS reactor, where superheated steam is injected to adjust the syngas H_2/CO ratio. An AGR unit then removes sulfur components, CO_2 and other minor species, and the resultant syngas is fed into a methanol reactor. A flash drum separates the

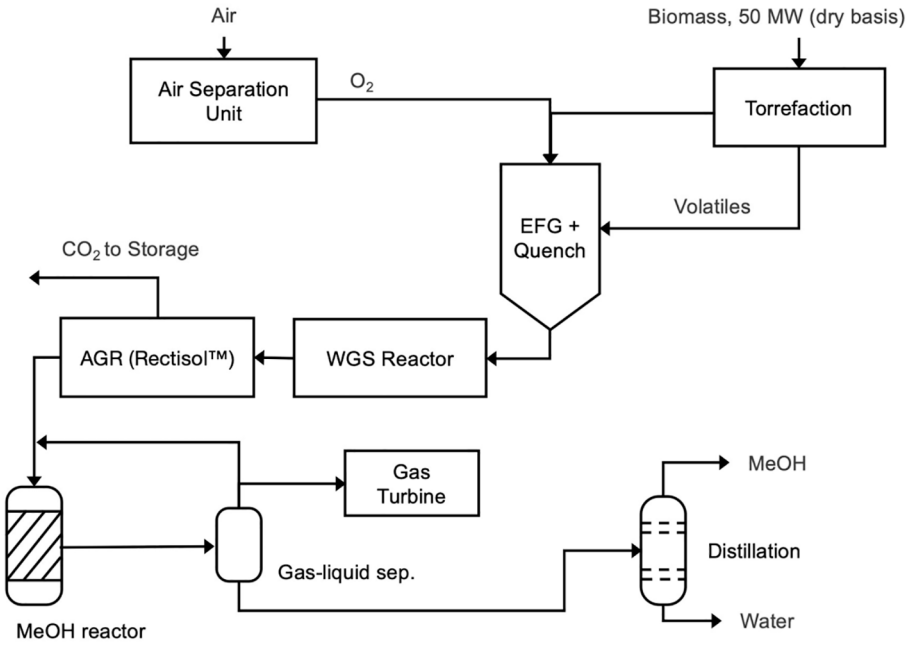

Fig. 1. Simplified biorefinery layout, System 1.

unreacted gases with the liquid product, which then passes through two distillation columns for purification, and 99.9% pure methanol is obtained.

The second modeled system S2, shown in Fig. 2, is similar to the first one. The main design difference is the introduction of an electricity-powered PEM water electrolyzer, to supply both O_2 and H_2. The oxygen flows to the entrained flow gasifier, replacing the ASU needed in the first system, while the hydrogen generation eliminates the need for a WGS reactor. Indeed, instead of supplying superheated steam during the WGS and subsequently removing large quantities of CO_2 to obtain a syngas suitable for methanol synthesis, the H_2/CO ratio is increased by injecting H_2 from the PEM electrolyzer. This has the effect of significantly improving the biorefinery performance, both in terms of overall energy efficiency and carbon conversion into the end-product.

As highlighted by other studies, a trade-off exists between capital costs and biomass transportation costs when establishing optimal biorefinery capacities [54]. Based on these considerations, and after comparison with similar studies, both biorefineries in this work are scaled to an input feedstock flow of 50 MW (based on biomass lower heating value). It is assumed large enough to benefit from economies of scale regarding investment costs, while ensuring minimal biomass transportation costs.

2.2.2. Modeling assumptions

Typically used commercial chemical engineering software packages can be time-consuming to construct. In this work, the approach of building simplified thermochemical models with Microsoft Excel and MATLAB was taken. There are many examples of similar approaches in the literature [55–58]. Key modeling components are described as zero dimensional with lumped parameters, as black boxes being fed by one or more inputs and returning one or more outputs. Steady-state operation is assumed for both systems. Mass and energy balance equations are defined for all components, each represented by a control volume, and molar compositions of the syngas are obtained at each step of the process. For some of the main processes (torrefaction, gasification, methanol synthesis), models including some kinetic or thermochemical aspects are developed. All components' models are calibrated with existing studies or available experimental data taken from literature before being implemented for the biorefineries of interest in this work.

For both systems, the main design process parameters and modeling methodology for the novel and most important process units are described. Main design process parameters for well-known units, frequently described in similar studies, as well as a more exhaustive list of assumptions for all units, can be found in the supplementary material along with references.

2.2.3. Design of system 1

During torrefaction, biomass is heated up to 300 °C in the absence of oxygen and under atmospheric pressure. During this process, the most reactive fraction of biomass (i.e. the hemicellulose fraction) is decomposed, so that torrefied wood and volatiles are formed. The torrefaction temperature was chosen based on better results reported in past studies [63,71], such as higher overall cold gas efficiency, higher energy content of volatiles, and shorter reaction times. The torrefaction model was built based on previous studies describing the solid and gaseous mass and energy yields as a function of temperature and time, given an input biomass composition [59–61]. A first step was setting up correlations describing the anhydric weight loss (AWL) of the input biomass, based on a kinetic model introduced by Di Blasi and Lanzetta, and validated with experimental data for torrefaction of wood [61–64]. The model describes the evolution of the torrefied product mass yield as a function of time, temperature, and a set of kinetic parameters taken from experimental data. The linear evolution of the torrefied solid elemental composition as a function of the previously obtained mass yield is then obtained, based on correlations fitted to experimental data [65,66]. From this result, the composition of the torrefaction volatile gases can be obtained from simple atomic balance, following the approach taken by Peduzzi et al. [67]. The compositions of initial and torrefied biomass, as well as the gaseous product, are presented in Table 1. An energy balance

Table 1
Biomass torrefaction, initial and final compositions (dry ash-free basis).

	Initial biomass	Torrefied biomass	Volatile gas
Relative mass (kg)	1	0.635	0.365
C %	50.23	61.60	30.45
H %	6.03	5.48	6.99
O %	43.0	32.92	60.53
N %	0.09	0.09	0.09
S %	0.01	0.01	0.01

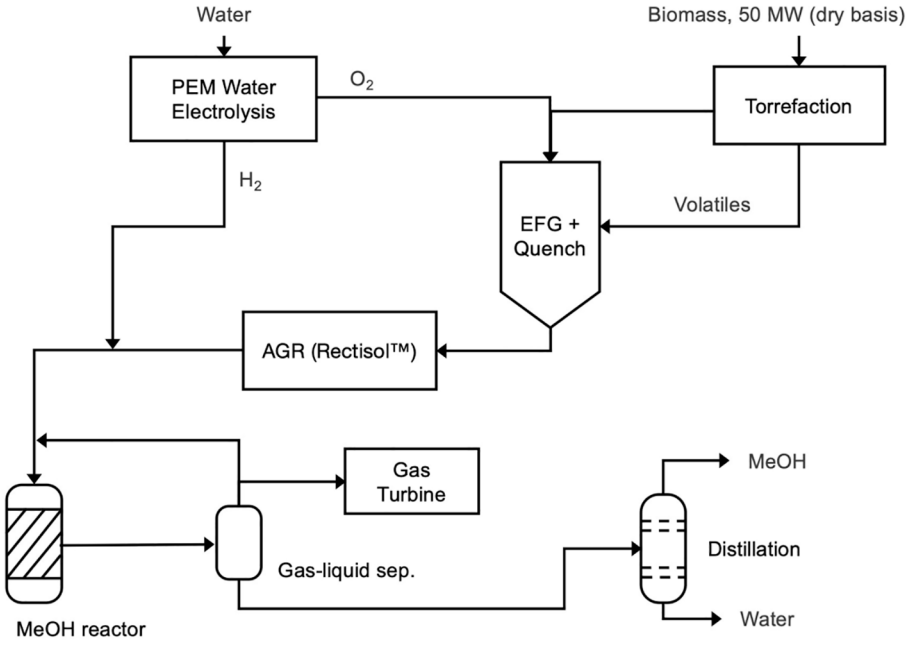

Fig. 2. Simplified biorefinery layout, System 2.

was then performed to determine the enthalpy of reaction, based on the calculation of standard enthalpies of formation and specific heat capacities of the torrefaction products at 300 °C. Finally, the energy yield and energy efficiency of the torrefaction process were found based on the heating values of the torrefaction products.

The torrefied wood powder is gasified by a dry-fed, oxygen-blown, entrained flow gasifier at a pressure of 45 bar and a temperature of 1300 °C [18,68]. The composition of the syngas obtained by this process depends on various factors, such as the type of biomass, the reactor design and operational conditions. The gasification temperature is high enough to assume sufficiently fast reaction kinetics, therefore the syngas composition after the gasification is determined by assuming chemical equilibrium at the exit temperature and pressure. Among the many equilibrium models available in the literature [69], the stoichiometric model introduced by Zainal et al. [70] was used here. The thermodynamic equilibrium can be represented by a set of equations with given known variables and a number of unknowns. The main gasification reaction, oxygen-blown, is the following:

$$CH_qO_rN_sS_t + fCO_2 + mO_2 \rightarrow x_1H_2 + x_2CO + x_3H_2O + x_4CO_2 + x_5CH_4 + x_6N_2 + x_7H_2S \quad (1)$$

The first term of the reaction can be replaced by this work's biomass of interest after torrefaction. f represents the number of moles of CO_2 per mol of input biomass, injected during the upstream feeding process. All carbon contained in the biomass is assumed to be converted, and the produced gas before quench is assumed to be a mixture of H_2, CO, CO_2, H_2O, CH_4, H_2S and N_2. The eight unknown variables m, x_1, …, x_7 are found by defining eight equations: five equations to represent the atomic balance equations, two equations defining the temperature-dependent equilibrium constants of a set of independent chemical reactions occurring in the gasifier, and one equation for the heat balance of the gasification process, assumed adiabatic. The latter is based on the enthalpies of reactants and products, at the gasification temperature. These equations are described in detail in the supplementary file. This system of equations is solved using MATLAB, and the final syngas composition as well as the oxygen input mass flow demand are obtained. The developed model was validated using previous studies' experimental and simulation results [18,70].

The quench of chemical volatiles is assumed to take place in the same gasification reactor. As described in Prins [71], "at high temperatures, the thermally unstable volatile gases from the upstream torrefaction step will decompose" into hydrogen, carbon monoxide, carbon dioxide and water, while dropping the syngas temperature. It is modeled assuming full stoichiometric conversion to H_2, CO, CO_2 and H_2O, and chemical equilibrium at exit conditions. The final syngas composition, after quench, is shown in Table 2:

The CO_2 captured from the main stream is compressed to 150 bar, and transported by pipeline to an underground storage facility. The pipeline's inside diameter is determined using the method introduced by McCoy and Rubin [72]. For the relatively short transport distances considered, no pump is needed along the pipeline. Assumptions are taken from the FE/NETL CO_2 Transport Cost Model [73]. The underground storage itself was not modeled, however associated costs are included in the system's economic assessment.

Table 2
Syngas composition after gasification and volatiles quench.

	mol/s	% mol
H_2	65.7	31.2
CO	107.8	51.2
CO_2	13.4	6.4
H_2O	23.6	11.2
CH_4	0.0	0.0
H2S	0.0	0.0
N_2	0.1	0.0

Methanol is synthesized by the following exothermic reactions:

$$CO + 2H_2 \rightleftharpoons CH_3OH \quad \Delta H^0 = -90.8\,kJ \bullet mol^{-1} \quad (2)$$

$$CO_2 + 3H_2 \rightleftharpoons CH_3OH + H_2O \quad \Delta H^0 = -49.6\,kJ \bullet mol^{-1} \quad (3)$$

The methanol synthesis unit is modeled assuming an approach to equilibrium. Methanol production can be estimated by solving the following system of equilibrium expressions, with n_i the number of moles of each species, n_T the total number of moles and P the reaction pressure. [74]:

$$K_{a1} = \frac{n_{CH_3OH}}{n_{CO}{n_{H_2}}^2}\frac{{n_T}^2}{P^2} \quad (4)$$

$$K_{a2} = \frac{n_{CO}n_{H_2O}}{n_{CO_2}n_{H_2}} \quad (5)$$

Both equilibrium constants K_{a2} and K_{a2} were taken from a study from Graaf and Winkelman [75] introducing temperature-dependent polynomial relationships fitted to experimental results for both reactions. Equilibrium conversion can thus be determined by defining x_1 as the moles of methanol formed and x_2 as the moles of water formed, and writing material balances around the reactor, $n_{X,i}$ being the initial number of moles of component X and n_T the total amount of moles in the mixture:

$$K_{a1} = \frac{\left(n_{CH_3OH,i} + x_1\right)}{\left(n_{CO,i} - x_1 + x_2\right)\left(n_{H_2,i} - 2x_1 - x_2\right)^2}\frac{\left(n_{T,i} - 2x_1\right)^2}{P^2} \quad (6)$$

$$K_{a2} = \frac{\left(n_{CO,i} - x_1 + x_2\right)\left(n_{H_2O,i} + x_2\right)}{\left(n_{CO_2,i} - x_2\right)\left(n_{H_2,i} - 2x_1 - x_2\right)} \quad (7)$$

This system of equations was implemented and solved in MATLAB. The heat release during the exothermic methanol synthesis was determined by an energy balance, given the standard enthalpies of Eq. (2) and (3).

2.2.4. Design of system 2

The second modeled biorefinery differs from the first in a few components. The PEM water electrolysis unit eliminates the need for both the ASU and the WGS unit, while the compression and transport of CO_2 to underground storage are not required as the very small amounts of removed CO_2 are vented.

The PEM electrolyzer converts water and electricity into hydrogen and oxygen. The unit is modeled as a black-box, given an input efficiency (LHV-based) and thus electrical consumption per unit of hydrogen produced. By stoichiometry, the amount of water and electricity needed for a required amount of oxygen or hydrogen can easily be determined. In this system specifically, the O_2 and H_2 required by biomass gasification and methanol production, respectively, are taken as inputs, and a certain amount of O_2 is produced as a surplus. This by-

product could be sold if it reaches a viable market, and its potential cost benefits are discussed later. The electrolyzer, under current assumptions, is assumed to be powered from the electricity grid, in order to have a continuous supply of electricity. This is assumed to benefit the system costs by aiming for a maximal capacity factor and a minimal capacity oversizing, lowering both the investment costs and levelized production costs. The key technical and economic assumptions are taken from the Hydrogen Analysis Production Models (H2A) documentation [26]. Among different scenarios included from the H2A models, conservative current (year 2019) technical values are chosen, while the impact of future PEM efficiency improvements is discussed later in the sensitivity analysis.

In order to increase the H_2/CO ratio for optimal methanol synthesis, the hydrogen supplied from the PEM electrolysis is injected and mixed to the syngas flowing out of the AGR unit. The methanol synthesis and gas–liquid separation models are the same as the ones used for the first system; however the unconverted syngas recycle ratio (88% recycle in the first system) is much higher in this design: 96%, as there is slightly less CO_2 in the syngas flowing out of the AGR unit. This high recycle ratio allows maximal methanol production efficiency, while ensuring an optimal H_2/CO ratio as well as a 3 mol% CO_2 fraction in the main input feed for optimal catalyst activity in the reactor.

2.3. Economic assessment

2.3.1. Main economic assumptions

The general economic assumptions used in the calculations in the following sections are presented in Table 3.

Capital costs were estimated using a bottom-up approach, with the module costing method introduced by Turton et al. [76] and accounting for contingencies and installation fees. Investment costs for CO_2 transport were computed with a different approach, using the FE/NETL CO_2 transport cost model [73]. The latter computes the total capital costs related to pipeline installation, for a given CO_2 flow and pipeline length. The annual capital repayment C_{ACR} allows expressing capital costs in a yearly value, accounting for depreciation over the expected lifetime of the plant (n years). It can be seen as the payment necessary to repay the loan contracted to build the plant. The biorefineries' total grassroots costs C_{GR} (total investment costs) are multiplied by a capital recovery factor expressed as:

$$C_{ACR} = C_{GR} \cdot \frac{d_e(1+d_e)^n}{(1+d_e)^n - 1} \tag{8}$$

with the effective discount rate d_e being the nominal discount rate d corrected for inflation i:

$$d_e = \frac{1+d}{1+i} - 1 \tag{9}$$

Similarly, the approach described in Turton et al. is used to determine operational (manufacturing) costs related to both biorefineries' operation. These are divided in direct costs (raw materials, utilities, operating labor, maintenance, etc.) and fixed costs (taxes, insurance, administration, etc.). Several direct costs depend on the biorefinery location, given chosen locations for the methanol demand point and the CO_2 storage site. These include costs related to the delivery of feedstock biomass from the roadside to the biorefinery, the delivery of the methanol end-product to the demand point, as well as the operational costs of the CO_2 pipeline transport and its storage underground. End-product methanol is assumed to be sold in the San Pedro Bay Port Complex (ports of Long Beach and Los Angeles, light blue in Fig. 3). The chosen CO_2 storage site is located in the Southern San Joaquin Basin [36], in Kern County (red area in Fig. 3).

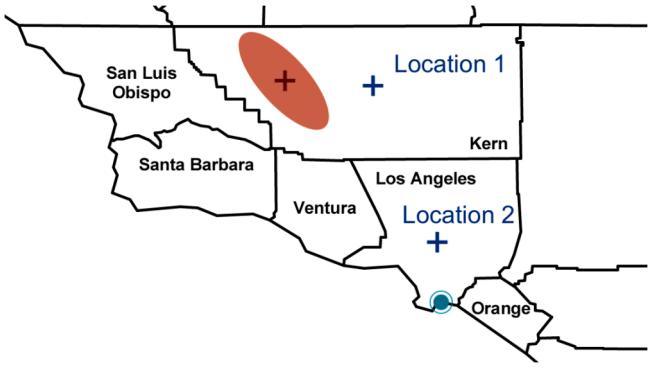

Fig. 3. Chosen biorefinery location scenarios.

Two scenarios, representing two locations each for both methanol production systems, are considered for comparison and introduced here. In the default scenario (location 1), the biorefinery is located in Kern County's centroid. This choice is motivated by its short distance to both the CO_2 storage site and San Pedro Bay Port Complex, while remaining close to available feedstock (forest residues) in the area. In the alternative scenario (location 2), the biorefinery is located in Los Angeles County's centroid, much closer to the demand point. Higher CO_2 pipeline transport costs and lower methanol transportation costs are expected. Biomass delivery cost is determined by assuming a mix of rail and truck transport: rail for inter-county transport, and truck for intra-county transport. Methanol distribution by rail or truck is comparable to other liquid fuels transportation in terms of handling requirements and costs [79,80]. For the relatively short distances considered in this study, truck transport is assumed to be more competitive than rail transport [81], thus the produced methanol is assumed to be transported by truck from the biorefinery to San Pedro Bay Port Complex. Transport unit costs found in the literature [36,82] are applied to both scenarios.

From yearly capital C_{ACR} and operational C_{OM} expenses, the levelized cost of production (LCOP) for both systems, in $/MWh, is obtained by normalizing the annualised costs by the yearly methanol output $\dot{m}_{MeOH,yr}$.

$$\text{LCOP} = \frac{C_{ACR} + C_{OM}}{\dot{m}_{MeOH,yr} \cdot LHV_{MeOH}} \tag{10}$$

A profitability analysis was then performed to track discounted cash flows during the biorefineries' expected lifetime. After the three-year construction time for the biorefinery, cumulative positive and negative cash flows (including revenues from selling the methanol product) are computed, and key economic results are determined. These include the project's net present value NPV, and the produced methanol's minimum fuel selling price MFSP to reach profitability. The latter is found by achieving a zero NPV at the end of the project lifetime. C_y is the net cash inflow-outflow during a year y including initial capital invested, n is the expected lifetime including construction time, and d_e the real discount rate. The list of assumptions is presented in Table 4 , taken from the literature [76,77].

$$NPV = \sum_{y=1}^{n} \frac{C_y}{(1+d_e)^y} \tag{11}$$

2.3.2. Sensitivity analysis & other scenarios

A local sensitivity analysis is performed over certain technical and economic parameters in order to understand their influence on both systems' levelized cost of production and minimum fuel selling price. Each of them was varied one-at-a-time, keeping all others at their nominal values. Two methods are used to set the range of values taken by each input variable. In the first one, all inputs' values are varied ± 30% around their nominal values, to be able to compare their relative impact on minimum fuel selling prices. In the second method, a different set of input variables' lower and higher bounds is chosen, to reflect more realistic scenarios; for instance, the CO_2 pipeline length varies from 25

to 60 miles in the first location scenario to cover the entire underground storage area shown in Fig. 3, and the higher bound of the PEM electrolyzer efficiency is based on future technology developments scenarios [26].

Other scenarios are also included when assessing the systems' economics. More specifically, the benefit of selling by-product O_2 and the impact of broader electricity purchasing cost variations on the second system's minimum fuel selling price, are evaluated. For the former, a conservative baseline value of \$60/ton O_2 is taken from Hank et al. [83], assuming a rate of 1.2 \$/€, along with low and high estimates of \$30/ton and \$90/ton O_2 for sensitivity.

2.3.3. CO_2eq abatement credits

According to Section 45Q of the Internal Revenue Code, for every ton of captured CO_2 intended to be either geologically sequestered or utilized, a tax credit can be claimed by the owner of the equipment [41]. Geological CO_2 sequestration includes storage in deep saline formations. Utilization includes "the use of such qualified carbon oxide for any other purpose for which a commercial market exists". Both modeled systems are eligible as their annual eligible amount CO_2 is greater than 25,000 metric tons. While System 1 would apply both for geological sequestration and utilization credits, System 2 would only apply for utilization. CO_2 credit amounts, in \$/tCO_2, depend on the storage medium and increase with time. They are applied to the annual quantities of CO_2 stored or utilized for both systems, and the yearly credits received are integrated into both systems' updated profitability analyses to determine new hypothetical minimum fuel selling prices. The method is then extrapolated to answer the following question: what is the minimal CO_2 tax value for which the methanol produced by both systems can be competitive with fossil fuels, synthetic fuels or other biofuels for shipping?

Another type of credits for which both biorefineries could be eligible are explicitly targeted at reducing the overall carbon footprint of transportation fuels. These reward projects producing fuels with a lower carbon intensity than conventional petroleum-based fuels. To be eligible for such credits, the lifecycle GHG emissions of the produced low-carbon fuel (accounting for its production, distribution and use) must be calculated and compared with conventional fuels. Credits are based on the difference in carbon intensity, measuring the GHG emissions reduction over the fuel lifecycle. As California LCFS credits do not apply to shipping fuels [40], it is assumed for the rest of the calculations that both systems are eligible for a generic GHG emissions reduction hypothetical credit, based on the comparison of their lifecycle emissions with those of traditional shipping fuels. The goal is to determine the impact of such credit on both systems' revenues and to determine the credit amounts at which the methanol produced in both systems becomes competitive with other shipping fuels. Well-to-haul emissions (including fuel production, distribution, storage and combustion) of conventional shipping fuels (MGO, HFO), as well as methanol produced from natural gas are computed from the GREET model [52]. Next, lifecycle GHG emissions of the methanol produced by both modeled systems is quantified to determine the emissions that could be avoided by switching to low-carbon methanol. These include all emissions associated with forest residue collection, chipping, storage, transportation, as well as all direct emissions associated with methanol production, distribution and combustion.

2.3.4. Shipping fuel demand estimation

In order to obtain a first approximation of the production scale needed to meet potential sustainable fuel demand in the San Pedro Bay Port Complex (ports of Los Angeles and Long Beach together) for medium-range shipping, an evaluation of the ports' current fuel consumption volumes was performed using public data obtained online. The fuel demand of Los Angeles and Long Beach ports together was approximated to 22.3 Trillion BTU, or 6.54 TWh. This corresponds to a 830 MW demand for ports of Los Angeles and Long Beach together, assuming a 0.9 yearly capacity factor.

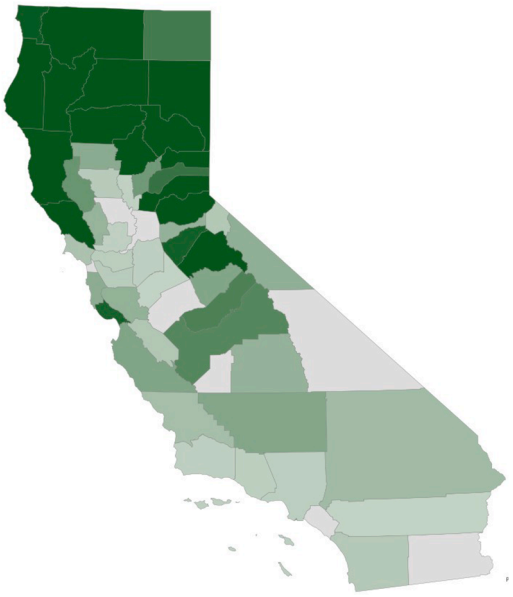

Fig. 4. Biomass feedstock, residues from forest management at a county-level. Darker green indicates high quantities, lighter green low quantities, grey no quantities [36,45] (For interpretation of the references to colour in this figure legend, the reader is referred to the web version of this article.)

3. Results

More detailed results, for all steps of the techno-economic assessment, can be found in the supplementary file.

3.1. Biomass supply assessment

A graphical representation of the quantities of forest residue available as a feedstock supply for this study are presented in Fig. 4. County-level quantities can be found in Baker et al [36]. The majority of the residues is found in Northern California (14.8 million ODMT/y estimated), with much less quantities available in Southern California (0.3 million ODMT/y estimated).

Following the methodology introduced in 2.1.2, a generic state-wide blend based on a weighted average of the dominant forest species determined previously is assumed to be collected, chipped, stored, transported and fed to the biorefinery. The computed proximate and ultimate analyses of this feedstock are presented in Table 5. The values presented here and chosen for this study are consistent with other values found in the literature. For example regarding heating values, Carvalho et al. [84] use a HHV of 20.5 MJ/kg and a LHV of 19.6 MJ/kg for a blend of hardwood and softwood residues wood chips, and Tan et al. [85] use a HHV of 19.9 MJ/kg and a LHV of 18.5 MJ/kg. Clausen et al. [18] use a LHV of 17.6 MJ/kg for willow wood chips, and Zhang et al. [24] 18.3 MJ/kg for sawdust. Wood chip moisture varies strongly from one study to another. Bisson and Han [86] use 27% moisture content after chipping hardwood and softwood tops, and Carvalho et al. use a moisture

Table 3
General economic assumptions.

	Value	Reference
Reference year	2019	
Expected lifetime (years)	25	[76]
Yearly availability	90%	[76]
Inflation rate	3%	[77]
Discount rate	8%	[78]

Table 4
Assumptions for the profitability analysis.

Fixed capital investment distribution	10% (year 1) 60% (year 2) 30% (year 3)
Working capital (M$)	0
Construction time (years)	3
Salvage value (M$)	0
Depreciation type	MACRS
Depreciation time (years)	5
Tax rate (%)	25.74
Effective discount rate (%)	4.85

Table 5
Input biomass ultimate and proximate analysis.

Ultimate Analysis (Dry Air)	
Carbon (%)	50.2
Hydrogen (%)	6.0
Oxygen (%)	43.0
Nitrogen (%)	0.1
Sulfur (%)	0.0
Ash (%)	0.7
Proximate Analysis (Dry Air)	
Fixed carbon (%)	15.3
Volatiles (%)	84.1
Ash (%)	0.7
HHV (MJ/kg)	20.0
LHV (MJ/kg)	18.7

Table 6
Costs related to biomass collection, chipping and storage.

Collection & chipping	$50/ODMT	[36]
Storage	$8.21/ODMT	[53]

Table 7
Costs related to biomass transportation.

Transportation, truck	$0.160/ODMT-mile	[36]
Transportation, rail	$0.079/ODMT-mile	[36]

Table 8
Current year (2019) GHG emissions related to biomass collection, storage and transportation.

Collection	16.4 $kgCO_2eq$/dry ton	[52]
Chipping	36.0 $kgCO_2eq$/dry ton	[36]
Storage	2.7 $kgCO_2eq$/dry ton	[53]
Transportation, truck Transportation, rail	93.4·10–3 $kgCO_2eq$/ton-mile	[52]
	21.5·10–3 $kgCO_2eq$/ton-mile	[52]

content of 35% for hardwood and softwood residues wood chips. For this study, woody residues moisture content is assumed to be 30%, for all forest types, a value taken from recent literature [36,87].

Costs of collecting, chipping and storing forest management residues are presented in Table 6. A few studies use similar costs for wood residue chips. Tan et al. [85] present roadside costs of $60/ODMT, the Billion-Ton Study [44] gives roadside costs of $60–80/ODMT, and Kizha and Han [88] a market price input price used for forest residues of $50/ODMT and costs for thinning operations (fire hazard reduction, forest restoration) from $26 to $52/ODMT. Biomass transportation costs are presented in Table 7.

Given the assumptions presented in Section 2.1.2, in Table 8 are presented the GHG emissions related to the collection (including thinning), chipping, storage and transport of forest management residues.

Table 9
Main modeling results for both biorefineries.

	System 1	**System 2**
Biomass input (MWth, dry-basis)	50	50
Biomass input (kg/s dry-basis)	2.68	2.68
Electricity consumption (MWel)	4.4	61.5
Electricity production (MWel)	4.4	4.9
Net electricity consumption (MWel)	0.0	56.6
MeOH output (MW, LHV)	33.4	66.1
MeOH output (kg/s)	1.68	3.32
Biomass-to-MeOH (%, LHV)	66.9	132.2
Biomass + Electricity-to-MeOH (%, LHV)	66.9	62.0
Carbon contained in input biomass (kg/s)	1.35	1.35
Carbon captured for underground storage (kg/s)	0.64	/
Carbon vented (kg/s)	/	0.05
Carbon in MeOH (kg/s)	0.63	1.25
Carbon in MeOH (% relative to input biomass)	47	92

3.2. Modeling of biorefineries

The main modeling results are presented in Table 9 for both systems. More detailed system flow diagrams, as well as the processes' molar and mass flows, can be found in the supplementary material. The overall efficiency of the second system, when considering its significantly high net electricity consumption, is lower than the first one. However, for an identical wood chips input flow, the second system yields nearly twice the amount of methanol produced by the first system, due to the hydrogen injection step. As biomass-to-methanol efficiencies are given relative to the input biomass in Table 9, the second system's efficiency is greater than 100% as the heating value of the injected hydrogen is included. The capacity of producing much more methanol from the same amount of input biomass allows for storing much more of its carbon in the end-product.

Sankey diagrams below (Figs. 5–8) illustrate the chemical energy flows and carbon flows for both modeled systems given in Table 9, including the efficiency losses along the main process units. Efficiencies are given relative to the input biomass prior to its torrefaction.

3.3. Economic assessment

3.3.1. Capital costs

Following the methodology introduced in Section 2.3.1, the grass-roots capital costs for both biorefineries were determined. The total amounts for both location choices are presented in Table 10. All costs are given in 2019 $. Constructing the biorefinery in the second location only affects the investment costs of the CO_2 pipeline used to transport it to the underground storage location, as its length significantly increases. Thus, capital costs for the first system increase. However, the capital costs of the second system, for which CO_2 is vented, are identical for both locations. When comparing both modeled systems' investment costs, their difference can primarily be explained by the replacement of the costly WGS and air separation units by a PEM electrolyzer, combined with the removal of the CO_2 compressor to 150 bar and the pipeline for its transportation.

3.3.2. Operational costs

The main results of the biorefineries' operational costs estimation are presented in Table 11, for both locations. The operational costs of both systems vary when changing the location of the biorefinery. This difference is due to the different distances from the biorefinery to biomass roadside, the methanol delivery demand point, and the CO_2 underground storage location. These will respectively impact the costs of biomass delivery, methanol delivery, and (for the first modeled system only) CO_2 transport. For the first system, the increased CO_2 transport and biomass delivery costs outweigh the lower methanol delivery costs. For the second system, the lower methanol delivery costs outweigh the higher biomass delivery costs. When comparing both systems, the main

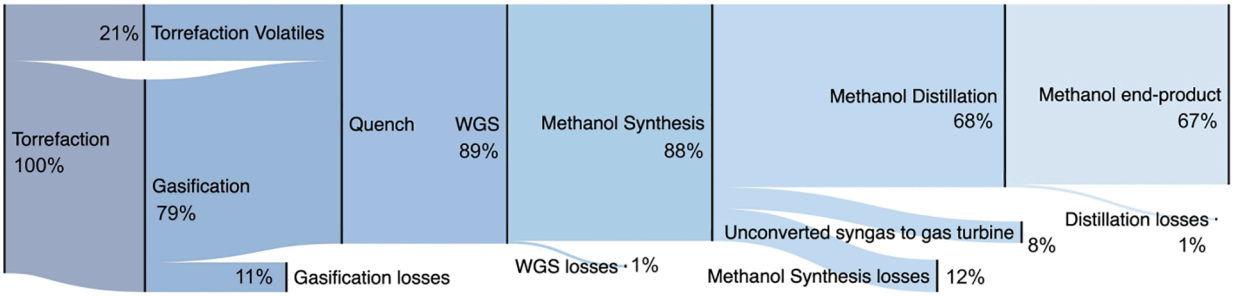

Fig. 5. System 1 - Chemical energy flow diagram, based on input biomass LHV.

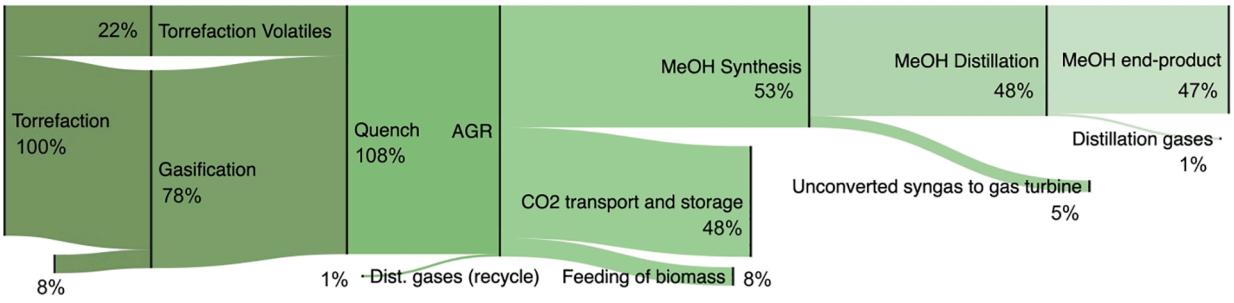

Fig. 6. System 1 - Carbon flow diagram, based on input biomass %C.

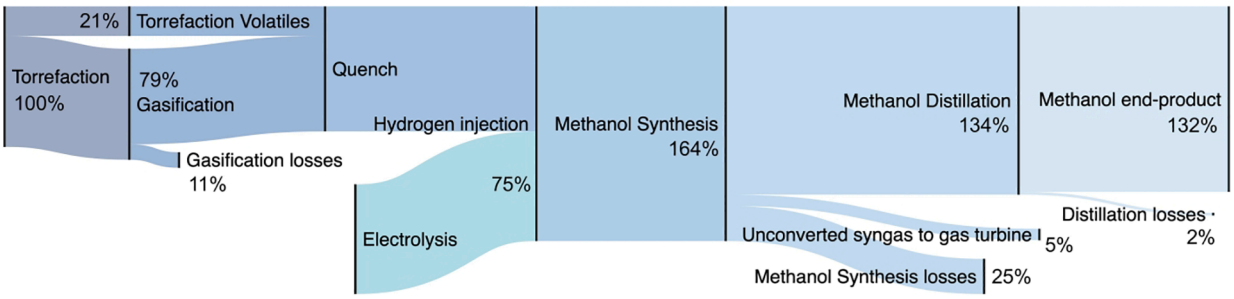

Fig. 7. System 2 - Chemical energy flow diagram, based on input biomass LHV.

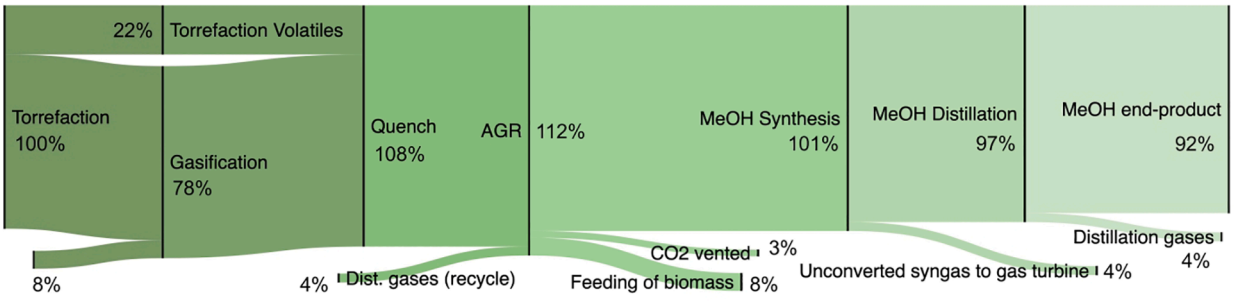

Fig. 8. System 2 - Carbon flow diagram, based on input biomass %C.

difference between their total operational costs is the purchase of electricity to power the electrolyzer in the second system.

3.3.3. *Levelized production costs*

By summing the annual capital repayment and total operational costs, the levelized costs of production were calculated for both systems and both locations, and are presented in Table 12. Despite having higher absolute yearly production costs than the first system, primarily due to much higher total operational costs, the second system's levelized production costs, in $ per methanol output, are lower thanks to the nearly doubled methanol yearly production.

Table 10
Capital expenses of both systems, for both locations.

	System 1		System 2	
	Location 1	Location 2	Location 1	Location 2
Capital Costs Total grassroots investment costs (M $)	116.9	126.1	112.9	112.9
Annual capital repayment (M $/year)	8.2	8.8	7.9	7.9

Table 11
Yearly operational expenses of both systems, for both locations.

	System 1		System 2	
	Location 1	Location 2	Location 1	Location 2
Operational Costs (M $/year)				
Direct costs	11.9	12.7	12.3	12.3
Raw materials/ utilities	8.2	8.2	26.3	25.7
Fixed costs and other general expenses	16.5	17.8	19.5	19.7
Total operational costs	36.7	39.0	58.2	57.6

Table 12
Levelized costs of production of both systems, for both locations.

	System 1		System 2	
	Location 1	Location 2	Location 1	Location 2
Yearly cost of production				
M $/year	44.8	47.9	66.1	65.6
Methanol annual production				
GJ/year	948,953	948,953	1,876,655	1,876,655
MWh/year	263,598	263,598	521,293	521,293
tons/year	47,686	47,686	94,304	94,304
million gallon/year	15.86	15.86	31.37	31.37
Levelized cost of production				
$/GJ	47.2	50.4	35.2	34.9
$/MWh	170.1	181.6	126.7	125.6
$/ton	940	1004	701	695
$/gallon	2.83	3.02	2.11	2.09

3.3.4. Profitability analysis

After applying the assumptions presented in Section 2.3.4, the sale of the produced methanol at specified prices allows computing the corresponding net present values over the project lifetime. Fig. 9 presents these results graphically, for both locations. The second system's NPV becomes positive for lower selling methanol prices than the first system. More generally, for methanol selling prices higher than $70 and $80/MWh (for locations 1 and 2 respectively), the second system's NPV is higher than the first system, as methanol revenues outweigh production costs. The increasing difference between both system's NPV for increasing methanol prices can be explained by the nearly doubled methanol output (thus revenue) in the second system. The minimum methanol selling price to reach a zero NPV is computed for all configurations, and given in Table 13. These are still much higher than current fossil methanol market prices, equal to $1.78/gallon for North America in September 2021 [89].

3.3.5. Sensitivity analysis

The sensitivity analysis results focus on the levelized cost of production for the first method, shown in Figs. 10 and 12, and the minimum fuel selling price for the second method, shown in Figs. 11 and 13. The parameter designating operational costs accounts for all variable and fixed expenses, including other varying parameters such as biomass and electricity costs. In the first method, for which all parameters are varied ± 30% from their nominal values (except for the capacity factor, physically capped at 1), the resultant levelized costs of production are displayed on the graph. The steepest lines represent the largest impact on the levelized cost of production or the most sensitive economic or technical parameters to the project's economic viability. For the second method, the parameters' nominal values are shown between brackets. Their respective lower and upper range bounds are displayed next to the horizontal bars representing their impact on the minimum fuel selling price, with the baseline value represented by a vertical line. Three input variables were chosen to be varied for the second location (L2), for which the baseline minimum fuel selling price is shifted to the right, according to results presented above.

3.3.6. Purchased electricity cost

As it can be seen in Fig. 13, the cost of purchased electricity considerably affects the economics of the second system, due to the electrolyzer's high electricity consumption. To better visualize its broader direct impact on the minimum fuel selling price, Fig. 14 presents the linear evolution of the MFSP as a function of the cost of purchased electricity, for the second system in the first location. For all

Table 13
Minimum fuel selling prices, for both systems and both locations.

	System 1		System 2	
	Location 1	Location 2	Location 1	Location 2
MeOH MFSP ($/MWh)	204	218	143	142
MeOH MFSP ($/gallon)	3.39	3.62	2.38	2.36

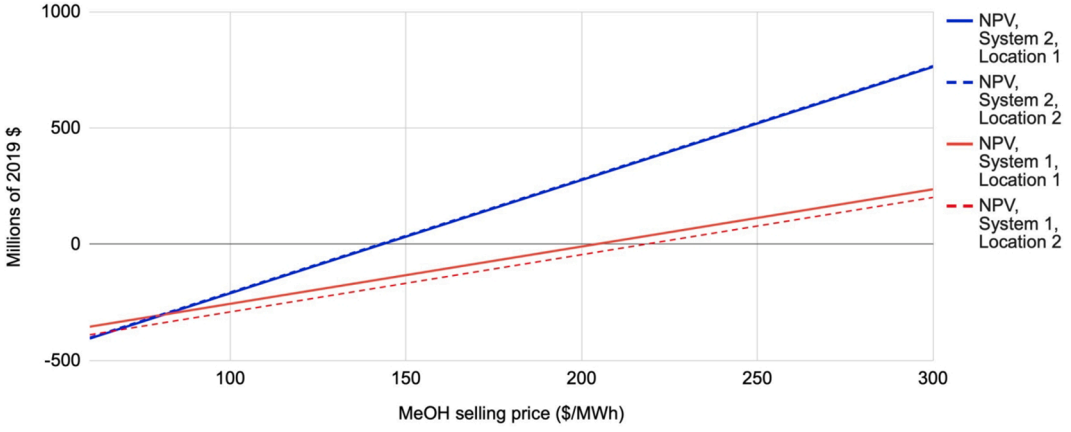

Fig. 9. Net present value of both systems over the project lifetime, for both locations.

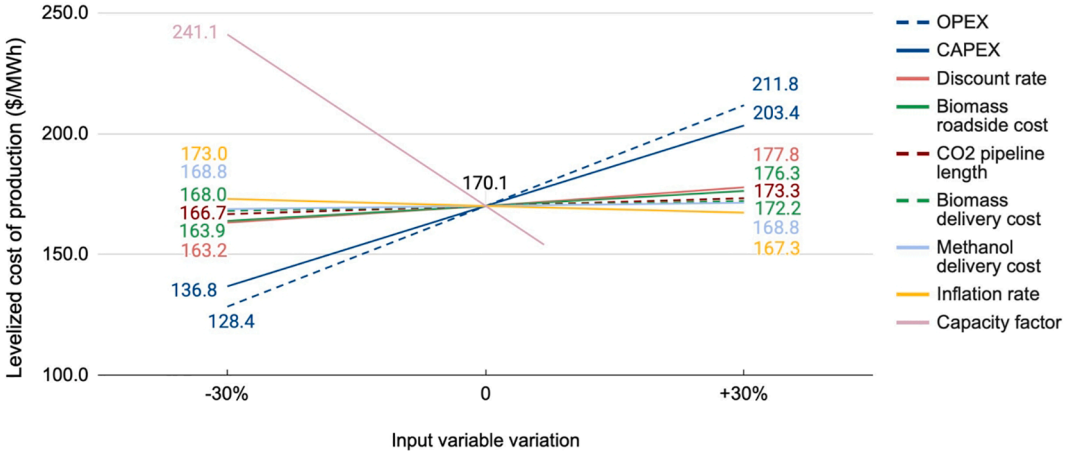

Fig. 10. System 1 - Sensitivity of levelized cost of production to varying input parameters (method 1).

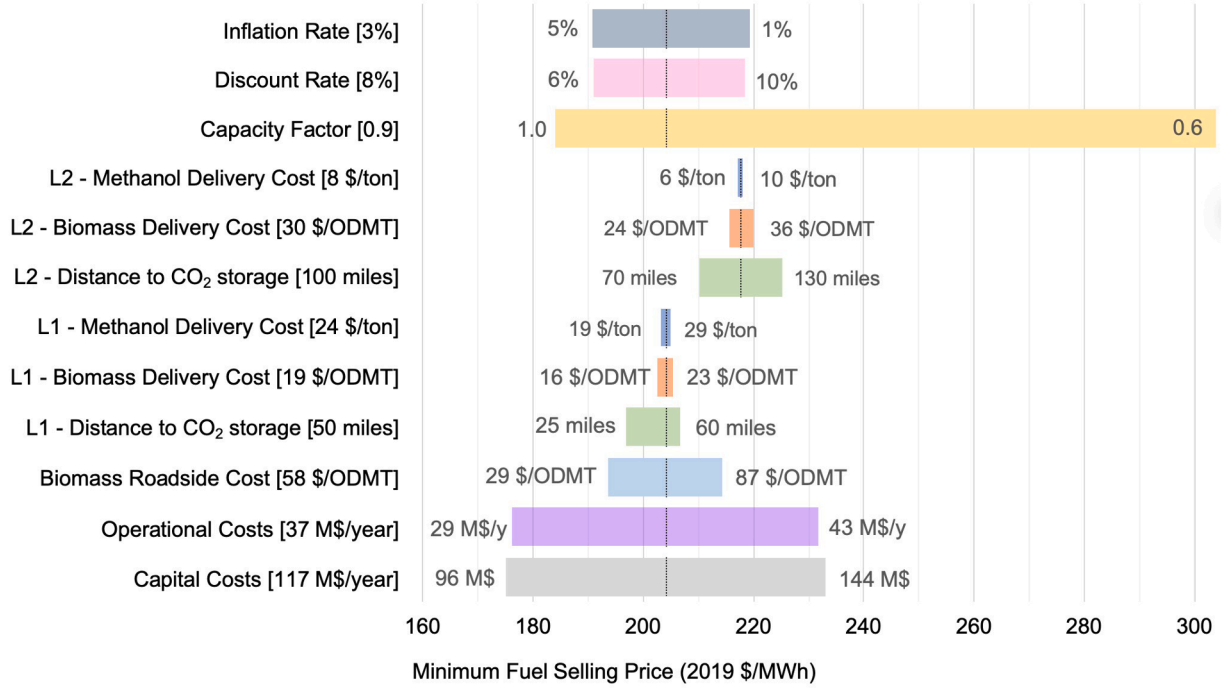

Fig. 11. System 1 - Sensitivity of MFSP to varying input parameters (method 2), for locations 1 (L1) and 2 (L2).

combinations of electricity and methanol costs beneath this line, the project is not economically viable, as the corresponding NPV would be negative.

3.3.7. CO_2eq abatement credits

3.3.7.1. Section 45Q credits. In Table 14, the impact of existing 45Q CO_2 tax credits on both systems' minimum fuel selling prices is shown. While the second system is eligible for utilization credits only, the first system additionally includes geological sequestration of the captured CO_2, for which credit amounts are higher. As a consequence the latter generates more revenue through these credits. Additionally, the first system's MFSP is inherently more sensitive to an increase in revenue than the second. Indeed, when comparing both systems, it is interesting to note that even though they store similar amounts of carbon dioxide per input biomass (either underground storage and in methanol in system 1, or in methanol in system 2), the amount of carbon dioxide stored per methanol output is higher for the first system. Hence, for a same credit amount variation, in $/t$CO_2$, its associated yearly revenue change will have a higher impact on the total revenues than for the second system. Thus, the first system's MFSP is more sensitive to the introduction of a 45Q CO_2 tax credit.

The impact of a range of hypothetical 45Q CO_2 tax credit values on both systems' minimum fuel selling prices is shown in Fig. 15. Both systems' MFSP are compared to a range of shipping fuel costs taken from the literature - fossil fuels (HSFO, VLSFO, MGO, LNG), biofuels (biodiesel, HVO, biofuel oil, bio-LNG) and synthetic fuels (hydrogen, ammonia) [90], shown on the graph. Similarly to what is observed in Table 14, the first system's economic viability is more sensitive to an increase of the credit amount.

3.3.7.2. Lifecycle GHG emissions reduction credits. The computed

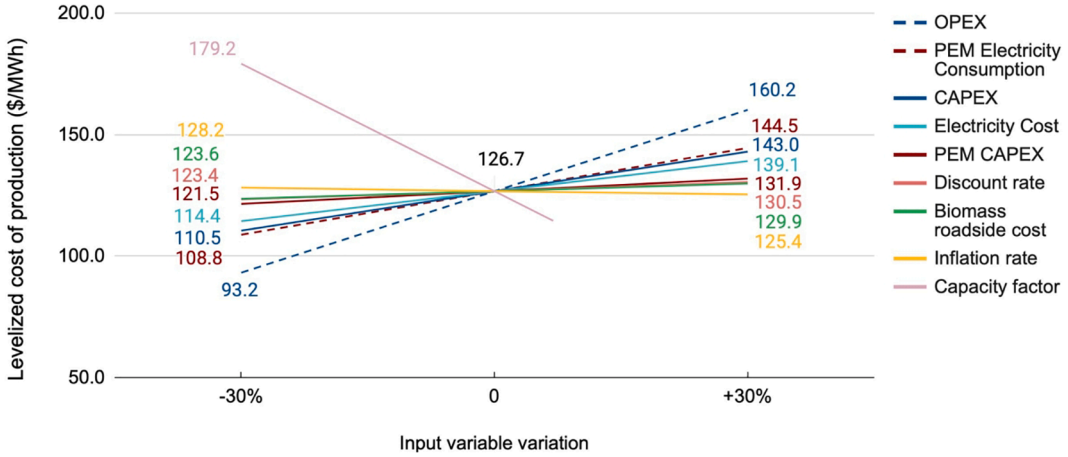

Fig. 12. System 2 - Sensitivity of levelized cost of production to varying input parameters (method 1).

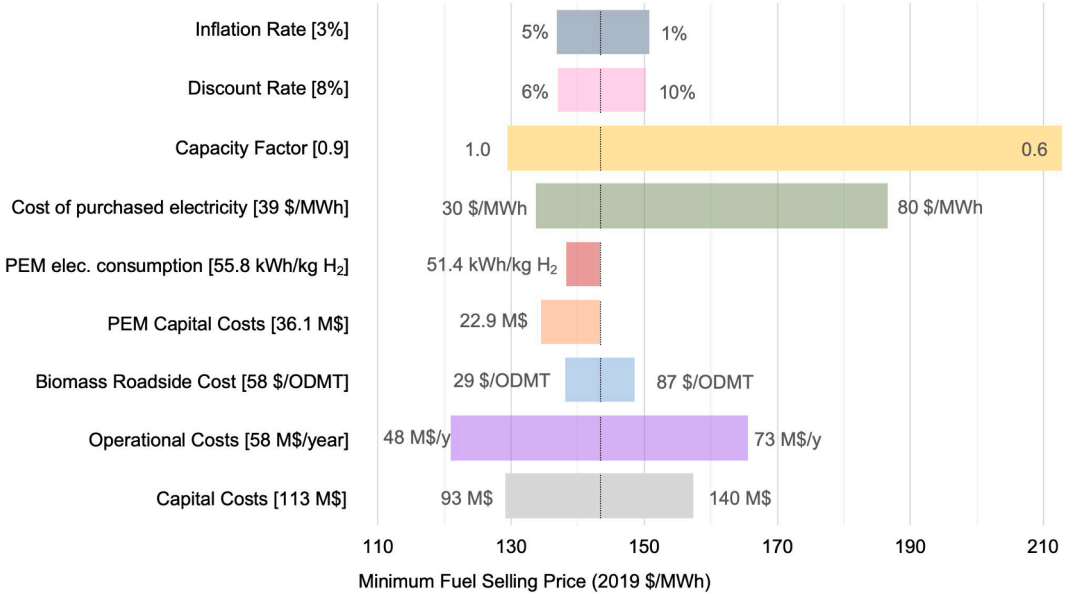

Fig. 13. System 2 - Sensitivity of MFSP to varying input parameters (method 2).

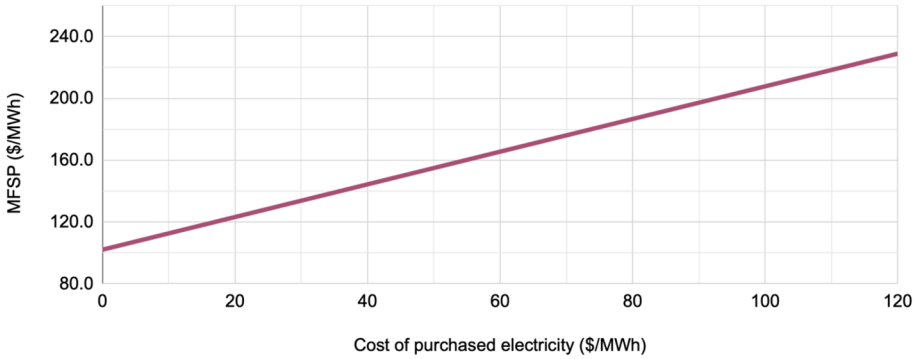

Fig. 14. System 2 - Impact of the purchased electricity cost on the minimum fuel selling price.

lifecycle GHG emissions for methanol produced by both modeled systems and conventional shipping fuels (as well as methanol produced from natural gas, for comparison), can be found in the Supplementary material. The yearly GHG emissions reduction, by switching to methanol produced by S1 or S2, are presented in Table 15. The large difference observed between both systems is explained by two main factors: the fact CO_2 is stored underground in the first system, and the large electricity consumption in the second system. If the captured CO_2 was vented instead of securely stored in the first modeled system, well-to-haul emissions would be positive and reductions compared to

Table 14
Impact of 45Q CO_2 tax credits on MFSP, for both systems and both locations.

	Location 1	Location 2	Location 1	Location 2
Baseline MFSP ($/MWh)	204	218	143	142
Updated MFSP ($/MWh)	191	205	138	137

conventional fuels would be in the order of 84–86%. For comparison, GHG emissions reduction values found in the literature, for studies that don't include underground storage of capture CO_2, range from 80% to over 95% for renewable methanol used as a marine fuel, compared to conventional shipping fuels [2,91,92].

The effect of the introduction of a hypothetical GHG emissions reduction credit for both systems' MFSP is shown in Fig. 16. The credits are here based on the lifecycle emissions reduction of methanol produced by systems 1 and 2, compared to the baseline lifecycle emissions of three shipping fuels: methanol produced from natural gas, HFO, and MGO. The obtained curve for S1 is similar to the one shown in Fig. 15, as the capture and storage/utilization of CO_2 represents a large portion of its lifecycle GHG emissions reduction. An additional factor that explains the higher sensitivity of the first system's MFSP to an increase in credit value is the much higher GHG emissions reduction in the first system due to the underground CO_2 storage and the zero-electricity consumption carbon footprint, compared to the second system. Storing CO_2 underground makes the produced methanol carbon-negative in System 1, and allows it to be competitive with fossil shipping fuels at lower credit amounts (≈$300/t$CO_2$eq).

3.3.7.3. Application of both types of credits. Assuming both systems are eligible to both CO_2 storage or utilization credits (on the basis of section 45Q credits) and hypothetical GHG emissions reduction credits (compared to MGO 0.1% Sulfur), their combined effect on the minimum

Table 15
GHG emissions reduction of methanol produced by both systems, compared to baseline fuels.

	Location 1	Location 2	Location 1	Location 2
GHG emissions reduction compared to MeOH from natural gas (NG) (% reduction)	162	162	38	39
HFO 0.1% sulfur (% reduction)	159	160	41	41
MGO 0.1% sulfur (% reduction)	164	165	36	36

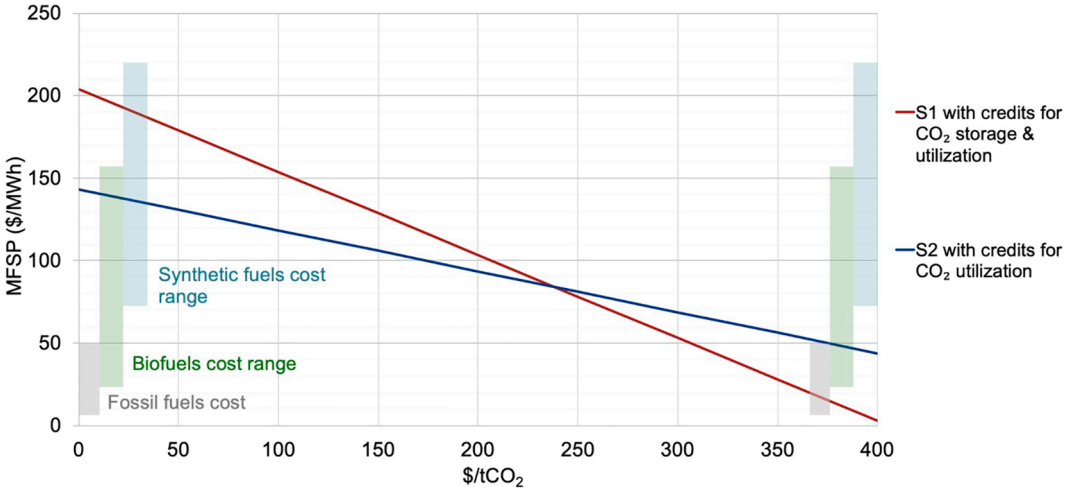

Fig. 15. Impact of hypothetical CO_2 storage/ utilization credits on MFSP, for both systems in Location 1.

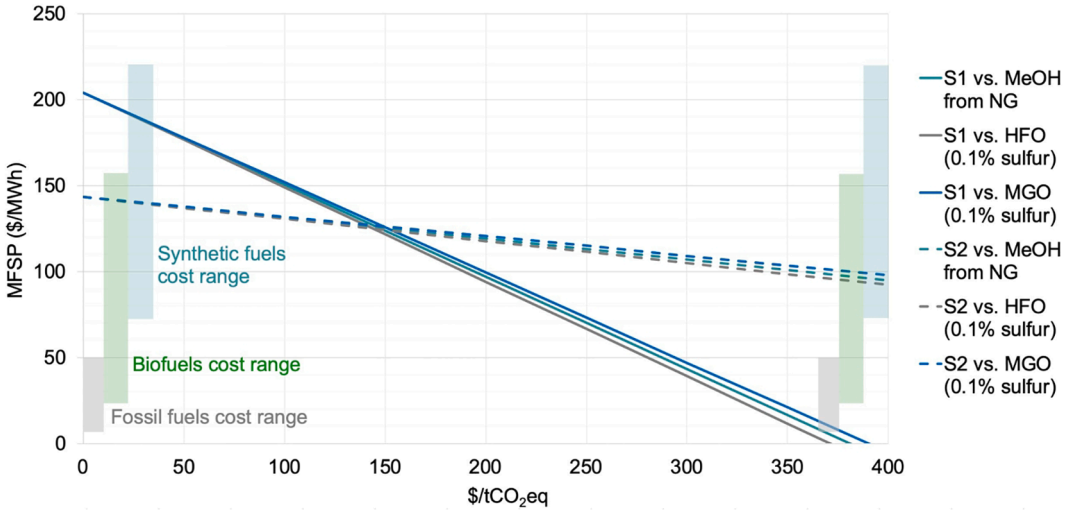

Fig. 16. Impact on MFSP of lifecycle GHG emissions reduction hypothetical credits compared to conventional shipping fuels and fossil methanol, for both systems.

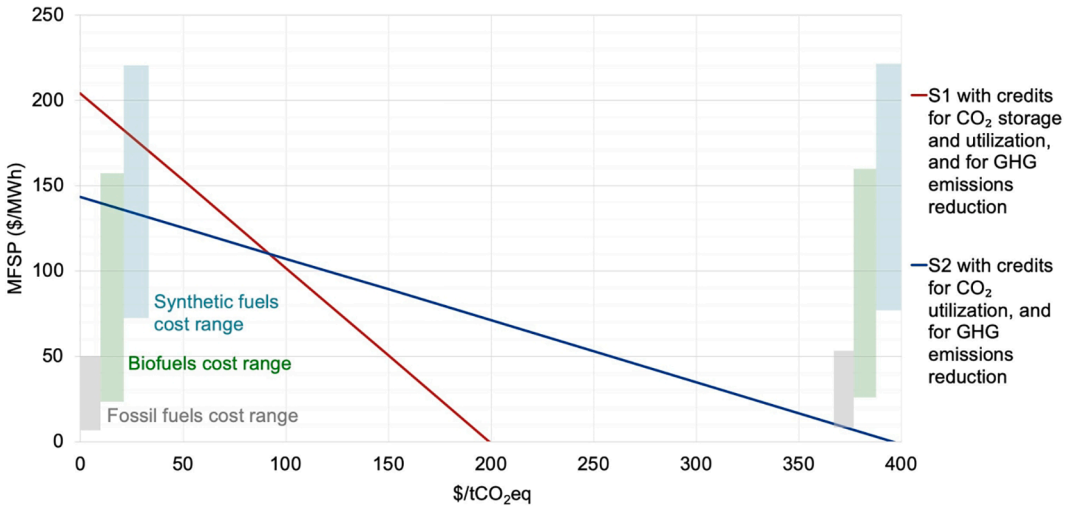

Fig. 17. Impact on MFSP of CO_2 storage/utilization credits and GHG emissions reduction credits, for both systems.

Table 16
San Pedro Bay Port Complex fuel demand, and feedstock biomass supply implications.

	System 1	System 2
Fuel demand met by a 50 MW biorefinery	4.0%	8.0%
Theoretical number of biorefineries needed to meet		
10% fuel demand	3	2
50% fuel demand	13	7
100% fuel demand	13	25
Theoretical amount of biomass needed to meet		
10% fuel demand (thousand ODMT/year)	189	96
50% fuel demand (thousand ODMT/year)	946	478
100% fuel demand (thousand ODMT/year)	1,893	956

methanol selling price can be evaluated by summing both credits' yearly revenues, and is represented in Fig. 17. The first modeled system would be competitive at much lower credit amounts primarily due to the fact it would be carbon-negative over its lifecycle.

3.3.7.4. Shipping fuel demand estimation. The methodology described in Section 2.3.7 allowed estimating the fuel demand for the ports of Los Angeles and Long Beach together: 394 million gallons of methanol. Assuming the system efficiencies presented above, the following results are obtained, shown in Table 16. These estimations are a starting point as they do not include some key economic factors, particularly regarding the supply of biomass. Meeting a significant portion of San Pedro Bay Port Complex's fuel demand by renewable methanol would require an large procurement of feedstock biomass from Northern California. This would necessarily increase the biomass transportation costs, as the largest quantities of forest residue are found in the most Northern counties.

4. Discussion

4.1. Modeling results

In terms of overall energy efficiency, when including the biorefinery's net electricity consumption, the first modeled system performs better than the second due to the large electrolyzer electricity consumption of the latter. However, the hydrogen injection allows a near doubling of the biomass-to-methanol efficiency compared to a system without electrolysis. This means that the second system is optimal when aiming for a maximal utilization of forest residues or when biomass is seen as a scarcer resource than electricity. This is relevant in the context of future grid build-out in California, when excess electricity might become more and more available with greater fractions of wind and solar generated power. If in the future there is greater access to cheap electricity, generating H_2 for methanol synthesis would be one form of power-to-liquid fuel storage, with the potential inexpensive long-term storage of a flexible biofuel that is liquid at ambient conditions. The obtained efficiency results are close to similar past studies. Clausen et al. [18,19] obtained overall efficiencies of respectively 63% and 62%, for systems similar to S1 and S2 (which reached efficiencies of respectively 67% and 62%), with vented CO_2 instead of storing it underground and alkaline electrolysis instead of PEM. Differences here arise from the input biomass composition and some model calculations assumptions. Carbon conversion efficiencies were found to be 44% and 96% for these systems, respectively, while S1 and S2 reached values of 47% and 92%, respectively. Yadav et al. [21] obtained an overall efficiency of 67% for a system similar to S1 without biomass torrefaction, and 69% for a novel process including chemical pre-treatment of biomass and changes in syngas cleaning and methanol synthesis. Butera et al. [29] obtained overall efficiencies ranging 37–71% for a flexible biomass-to-methanol system integrating solid oxide cells operating either in electrolysis mode or fuel cell mode, and carbon conversion efficiencies up to 92%. Zhang et al. [24] obtained an overall efficiency of 66% for a system resembling S2 but with no biomass torrefaction and solid-oxide electrolysis rather than PEM electrolysis.

4.1.1. Economic results

If revenues for both systems are only comprised of the sale of end-product methanol and do not include additional revenue streams such as CO_2eq abatement credits or the sale of by-product O_2, the second system is more profitable than the first for methanol selling prices above $80/MWh. Indeed, the economic results have shown that despite having higher absolute production costs, the second modeled system's levelized production costs, in $/MWh, are lower than the first, due mainly to the much higher methanol yield. The choice of biorefinery location directly impacts some of its operational costs. The first modeled system is particularly more affected by this choice, as costs related to CO_2 transport (proportional to the distance to the underground storage site) represent a significant portion of total costs. Here, being located in Kern County is the most attractive option mainly due to the proximity to the CO_2 storage area. For the second system however, the difference between the delivery costs of biomass and methanol is not large enough for one the locations to be significantly beneficial.

It is difficult to compare cost results between studies due to the large number of assumptions involved. However, it is still interesting to mention them for comparison. Typical annualized investment cost

gathered from existing similar biomass-to-methanol projects range from $37 to $53/MWh [6]. For comparison, S1 and S2 investment costs amount to respectively $56 and $28/MWh, using similar economic assumptions. According to Butera et al. [25], the first commercial forest biomass gasification-to-methanol plant, operating in Sweden, had investment costs of 250 M$, for a biomass input of 110 MWth. For production costs, Tock et al. [14] found levelized production costs ranging from $145 to $188/MWh for 20 MW systems, and from $104 to $137/MWh for 400 MW systems, all similar to results for S1 ($170/MWh). Conti [16] obtained production costs of $178/MWh for 50–100 MW biorefineries similar to S1, assuming a rate of 1.2 $/€. More recently, production costs found in Butera et al. [25] for a modeled system similar to S2, with SOEC instead of PEM, amount to $91/MWh. The main reason explaining the difference with the results for S2 ($127/MWh) are a lower electricity price, and lower estimated investment costs, due to economies of scale as the biorefinery size is much larger (400 MW). Finally, Zhang et al. [24] obtained production costs ranging from $98 to $139/MWh, depending on the scenario, for a modeled system similar to S2.

Sensitivity analysis results have shown that both systems' levelized costs of production and minimum fuel selling prices were sensitive to a range of technical or economic input parameters. More specifically, the yearly availability of the biorefinery plays a major role in the final economics of the project for both systems. The first system's economics are very sensitive to a variation of capital costs, as these represent a larger fraction of total costs, compared to the second system. As discussed above, the distance to the CO_2 storage site is also critical. The second system's economics are particularly sensitive to the cost of electricity, given the large electrolyzer consumption. Future H2A scenarios predicting lower capital costs and higher efficiencies for PEM technology could also significantly bring down overall production costs. Finally, the introduction of a price for by-product O_2 sold would lower its minimum fuel selling price by adding an additional revenue stream. While the effect of a combination of inputs' variations on the project economics has not been studied, their cumulative impact on the methanol production costs are expected to be generally additive.

Both modeled systems could be eligible today for existing 45Q CO_2 tax credits. However, even though their amount was recently increased and their eligibility scope enlarged to include CO_2 utilization, their values remain too low to significantly reduce the minimum fuel selling prices. With the assumptions taken, the produced methanol would only become competitive compared to conventional fossil shipping fuels at much higher credit amounts of $300 to $400/t$CO_2$. The minimum fuel selling price of the first system is more sensitive to an increase of CO_2 credit amounts, and for credits higher than $240/t$CO_2$, the first system would become economically favorable. Furthermore, the methanol produced in the first system is carbon-negative after calculating its lifecycle emissions from feedstock collection to final delivery. Indeed, the biogenic credit applied to the biomass and the geological sequestration of CO_2 more than offsets lifecycle emissions related to feedstock, conversion, distribution and shipping combustion, resulting in net negative GHG emissions. In comparison, the methanol produced by the second system has a positive overall carbon footprint, mainly due to its large electricity consumption. Thus, a scenario including GHG emissions reduction credits would mostly favour the costs of methanol produced with the first system. For credits higher than $150/t$CO_2$eq, the first system would become economically more attractive. If a biorefinery were eligible for both 45Q and GHG reduction credits, the same results are seen. Assuming they have the same value for simplification, for credits higher than $90/t$CO_2$, the first system would be more competitive than the second. In this case, the methanol produced with systems 1 and 2 would become competitive compared to conventional fossil shipping fuels at credit amounts of respectively $150 and $250/t$CO_2$eq approximately.

Finally, it was found that the forest residues quantities evaluated in Baker et al., and used for this study, would be theoretically sufficient to meet the approximated shipping fuel demand of the San Pedro Bay Port Complex for medium-range freight.

4.1.2. Limitations

Some of the limitations of the present study, that could be the basis for future work, are addressed here. First, this study neglects any competition for the storage of CO_2. Yet, more and more CCS projects such as direct air capture or enhanced oil recovery are likely to compete for saline aquifers or depleted reservoirs in the future. This aspect could be taken into account and also points to the need for further regulatory development in this area. Furthermore, costs related to methanol bunkering were neglected, as the supply chain considered ends after methanol delivery to the port. For a more comprehensive assessment of the overall costs required to switch from fossil shipping fuels to methanol, future work should include capital and operational expenditures of retrofitting bunker vessels as well as fuel handling and storage facilities. Moreover, future work should implement a detailed constrained optimization when assessing biomass delivery costs to the biorefinery. It would take into account competition for forest residue usage for transportation biofuels production and heat and power generation for instance, and lead to more realistic constraints for this feedstock procurement. One could also enhance precision in the calculation of the distance from forest roadside to the biorefinery, by identifying the exact locations of biomass roadside points, instead of county centroids. This would require detailed spatial data on the forest residue quantities, instead of aggregated county-level amounts. While this study focused on modeling a single 50 MW biorefinery in two potential locations, future work could also assess multiple methanol production systems and optimize their location and capacity to minimize total costs, given several spatial constraints such as biomass availability, road or rail lines, underground CO_2 storage locations and delivery end-points. This would for instance allow evaluating the relevance of using more of Northern California biomass, or delivering methanol to Northern California ports. The scenarios considered in this work are based on current (2019) economic assumptions such as estimated equipment capital costs, price of electricity, or other operational expenses. Detailed sensitivity analysis is provided, including future technical and cost developments, particularly for PEM electrolysis. More detailed scenario development for the future is an area for further work. These would be relevant in the context of long-term decarbonization policies in the areas of transportation and shipping fuels more specifically. Grid electricity was chosen to power continuously the electrolyzer in the second modeled system, allowing a high yearly availability. In the context of increasing renewable electricity production in California and increasing periods of oversupply from intermittent sources, some future work should additionally integrate granular curtailment data from renewable sources to model a PEM electrolyzer powered by cheap clean electricity when it is available, combined with hydrogen storage to maintain operation (and high capacity factors) when electricity is not available. This would leverage the full advantages of PEM technology, specifically its ability to operate dynamically. It would subsequently allow significant reductions in the second modeled system's carbon footprint and the generation of more GHG emissions reduction credits, while storing renewable energy in the form of biofuels. Finally, the use of cleaner road transportation modes for biomass and methanol delivery, such as fuel cell trucks powered by green hydrogen for instance, could be included in future work to further reduce the methanol product lifecycle emissions.

5. Conclusion

In this study, a techno-economic and environmental assessment of renewable methanol produced by gasification of forest residue in California was performed. Two biorefinery systems were first modeled thermodynamically, extending past work to integrate some important design changes. Next, a bottom-up assessment of the supply chain investment and operational costs, from the collection of forest residue to

the delivery of end-product methanol, was performed for the two system designs at two biorefinery location scenarios considering spatial constraints and California-specific economic assumptions. A profitability analysis to determine the minimum fuel selling price over the project lifetime was then carried out followed by a sensitivity analysis to evaluate the influence of key technical and economic parameters on the project economics. Based on the assessment of the amounts of CO_2 stored and utilized throughout the production of low-carbon methanol, as well as the methanol product lifecycle GHG emissions, the impact of introducing CO_2eq abatement credits on the methanol minimum selling price was then evaluated for all scenarios. Finally, a high-level estimation of the portion of shipping fuel demand met by these methanol production pathways was estimated for medium-range shipping at the San Pedro Bay Port Complex in Southern California. Based on this work, the following conclusions are drawn:

- Renewable methanol from forest residue gasification can achieve substantial GHG emissions reductions in California. Compared to traditional shipping fuels or fossil methanol, abated lifecycle emissions, in gCO_2eq/MJ of fuel, range from 38 to 165%, depending on the system and scenario considered. This corresponds to annual quantities of 59 to 145 $ktCO_2eq$/year for a 50 MW biorefinery, equivalent to 32–153 gCO_2eq/MJ abated. If biomass gasification is coupled with water electrolysis, methanol production is nearly doubled, reaching 1.32 J of methanol per J of biomass LHV-based and 92% carbon conversion. In this case, overall lifecycle emissions are largely dependent on the carbon intensity of the electricity supply with the overall carbon balance being neutral at best.
- Greater GHG reductions and net negative carbon emissions are achieved when methanol production includes geological CO_2 sequestration of 48% of the carbon initially contained in the wood chips in system 1. This represents negative emissions of −71 gCO_2eq/MJ. Net GHG emissions along the product lifecycle then amount to −57 gCO_2eq/MJ, as the carbon uptake during initial biomass growth virtually offsets methanol combustion emissions. The capital and operational costs of this CO_2 capture, transport and storage represent a small fraction of total costs (6–8% of levelized production costs together, depending on the biorefinery location) in part due to the proximity of the biorefinery to the storage site.
- Carbon-negative or low-carbon methanol produced by the first and second modeled system is currently not economically competitive with conventional or alternative shipping fuels. Estimated minimum selling prices to reach positive net present values range from $142 to $218/MWh, compared to current fossil methanol price of about $108/MWh and conventional shipping fuel prices ranging from $10 to $50/MWh. The lower range is obtained with methanol produced by biomass gasification coupled to PEM electrolysis, thanks to the increased methanol yield. However, the introduction of CO_2eq abatement incentives such as Section 45Q federal tax credits or LCFS-like credits could bring minimum fuel selling prices down significantly, particularly when methanol production includes geological CO_2 sequestration. In this case, the produced methanol can become competitive with fossil shipping fuels at carbon credit values ranging from $150 to $300/$tCO_2eq$, depending on the eligible credits.
- The forest residue quantities available in California would be sufficient for renewable methanol production to meet a significant portion of a major American port's fuel demand. More specifically, even if much lower than in Northern California, the forest residue quantities available in Southern California could potentially meet 30% of the San Pedro Bay Port Complex fuel demand for medium-range shipping, when considering methanol production system 2. This production scale is met by four 50 MW biorefineries.

In some future work, additional scenarios taking into account economies of scale, and more detailed future technology and cost developments, should be studied to assess the renewable methanol production at scale for California.

CRediT authorship contribution statement

Nicolas de Fournas: Conceptualization, Methodology, Software, Validation, Formal analysis, Investigation, Writing – original draft, Visualization. **Max Wei:** Conceptualization, Resources, Writing – review & editing, Supervision.

Declaration of Competing Interest

The authors declare that they have no known competing financial interests or personal relationships that could have appeared to influence the work reported in this paper.

Acknowledgements

This research was supported by the U.S. Department of Energy's Office of Energy Efficiency and Renewable Energy under Contract No. DE-AC02-05CH11231. N.d.F. would like to express his gratitude to his supervisor at ETH, Prof. Dr. Christoph Müller, for his support.

Appendix A. Supplementary data

Supplementary data to this article can be found online at https://doi.org/10.1016/j.enconman.2022.115440.

References

[1] Gielen D, Castellanos G, Ruiz C, Roesch R, Ratka S, Sebastian T, "Study Navigating the Way to a Renewable Future–Solutions to Decarbonise Shipping: Preliminary findings for the UN Climate Action Summit 2019," 2019.
[2] Hawkins TR, Zaimes GG, "Biofuels for Marine Applications: Environmental Considerations," 2020.
[3] Faber S, Hanayama S, Zhang S, Pereda P, Comer B, Hauerhof E, Kosaka H, Fourth IMO GHG study 2020, 2020.
[4] Mukherjee A, Bruijnincx P, Junginger M. A perspective on biofuels use and CCS for GHG mitigation in the marine sector. Iscience 2020;23(11):101–758. https://doi.org/10.1016/j.isci.2020.101758.
[5] Smith T, Raucci C, Hosseinloo SH, Rojon I, Calleya J, De La Fuente SS, et al. CO_2 emissions from international shipping. Possible reduction targets and their associated pathways. London, UK: UMAS; 2016.
[6] International Renewable Energy Agency, "Innovation Outlook : Renewable Methanol," 2021. [Online]. Available: https://www.irena.org/publications/2021/Jan/Innovation-Outlook-Renewable-Methanol.
[7] S&P Global Platts, Changing tack, Oct. 2020. [Online]. Available: https://www.spglobal.com/platts/en/marketinsights/special-reports/shipping/changing-tack-floating-storage/.
[8] Lloyd's Register, Methanol Bunkering, Technical Reference, Jul. 2020. [Online]. Available: https://vpoglobal. com/wp-content/uploads/2020/09/Introduction_to_Methanol_Bunkering.pdf/.
[9] DNV GL, *Alternative Fuels Insight*, Jul. 2020. [Online]. Available: https://afi.dnvgl.com/Statistics.
[10] Orsted, *Leading Danish companies join forces on an ambitious sustainable fuel project*, May 2020. [Online]. Available: https://orsted.com/en/media/newsroom/news/2020/05/485023045545315.
[11] Julia Horowitz, CNN Business, Maersk just ordered 8 carbon neutral ships. Now it needs green fuel, Aug. 2021. [Online]. Available: https://edition.cnn.com/2021/08/24/business/maersk-carbon-neutral-ships/index.html.
[12] Abigail Martin, *A step forward for green methanol and its potential to deliver deep GHG reductions in maritime shipping*, Sep. 2021. [Online]. Available: -ghg-reductions-marine-sept21.
[13] Haraldson L. Methanol as fuel. Methanol as Fuel & Energy Storage Workshop. Lund Sweden. 2015.
[14] Tock L, Gassner M, Maŕechal F. Thermochemical production of liquid fuels from biomass: Thermo-economic modeling, process design and process integration analysis. Biomass Bioenergy 2010;34(12):1838–54. https://doi.org/10.1016/j.biombioe.2010.07.018.
[15] Andersson J, Lundgren J, Marklund M. Methanol production via pressurized entrained flow biomass gasification–techno-economic comparison of integrated vs. stand-alone production. Biomass Bioenergy 2014;64:256–68. https://doi.org/10.1016/j.biombioe.2014.03.063.
[16] Conti D, Harahap F, Silveira S, Santasalo-Aarnio A. A techno-economic assessment for optimizing methanol production for maritime transport in Sweden. In: 32nd International Conference on Efficiency, Cost, Optimization, Simulation and Environmental Impact of Energy Systems, ECOS 2019, 23-28 June 2019, Wroclaw, Poland. Institute of Thermal Technology; 2019. p. 4703–12.

[17] Clausen LR, Elmegaard B, Houbak N. Design of novel DME/methanol synthesis plants based on gasification of biomass. Copenhagen, Denmark: Danish Technical University; 2011.

[18] Clausen LR. Integrated torrefaction vs. external torrefaction–a thermodynamic analysis for the case of a thermochemical biorefinery. Energy 2014;77:597–607. https://doi.org/10.1016/j.energy.2014.09.042.

[19] Clausen LR. Maximizing biofuel production in a thermochemical biorefinery by adding electrolytic hydrogen and by integrating torrefaction with entrained flow gasification. Energy 2015;85:94–104. https://doi.org/10.1016/j.energy.2015.03.089.

[20] Liu Y, Li G, Chen Z, Shen Y, Zhang H, Wang S, et al. Comprehensive analysis of environmental impacts and energy consumption of biomass-to-methanol and coal-to-methanol via life cycle assessment. Energy 2020;204:117961. https://doi.org/10.1016/j.energy.2020.117961.

[21] Yadav P, Athanassiadis D, Yacout DM, Tysklind M, Upadhyayula VK. Environmental impact and environmental cost assessment of methanol production from wood biomass. Environ Pollut 2020;265:114–990. https://doi.org/10.1016/j.envpol.2020.114990.

[22] Clausen LR, Houbak N, Elmegaard B. Technoeconomic analysis of a methanol plant based on gasification of biomass and electrolysis of water. Energy 2010;35(5):2338–47. https://doi.org/10.1016/j.energy.2010.02.034.

[23] Larose S, Labrecque R, Mangin P. Electrifying with high-temperature water electrolysis to produce syngas from wood via oxy-gasification, leading to superior carbon conversion yield for methanol synthesis. Appl Sci 2021;11(6):2672. https://doi.org/10.3390/app11062672.

[24] Zhang H, Wang L, Pérez-Fortes M, Van herle J, Maréchal F, Desideri U. Techno-economic optimization of biomass-to-methanol with solid-oxide electrolyzer. Appl Energy 2020;258:114071. https://doi.org/10.1016/j.apenergy.2019.114071.

[25] Butera G, Jensen SH, Ahrenfeldt J, Clausen LR. Techno-economic analysis of methanol production units coupling solid oxide cells and thermochemical biomass conversion via the TwoStage gasifier. Fuel Process Technol 2021;215:106–718. https://doi.org/10.1016/j.fuproc.2020.106718.

[26] James B et al., "Analysis of Advanced H_2 Production & Delivery Pathways," Project ID P, vol. 102, p. 22,.

[27] Holmgren K, *Investment cost estimates for gasification-based biofuel production systems*, 2015.

[28] Clausen LR, Elmegaard B, Houbak N. Technoeconomic analysis of a low CO_2 emission dimethyl ether (DME) plant based on gasification of torrefied biomass. Energy 2010;35(12):4831–42. https://doi.org/10.1016/j.energy.2010.09.004.

[29] Butera G, Jensen SH, Gadsbøll RØ, Ahrenfeldt J, Clausen LR. Flexible biomass conversion to methanol integrating solid oxide cells and TwoStage gasifier. Fuel 2020;271:117–654. https://doi.org/10.1016/j.fuel.2020.117654.

[30] Zomer G, Finner S, Harmsen J, Vredeveldt A, van Lieshout P. Green Maritime Methanol; operation aspects and the fuel supply chain. TNO: Tech. Rep; 2020.

[31] NTU Maritime Energy and Sustainable Development Centre of Excellence, "Methanol as a marine fuel – availability and sea trial considerations," 2021. [Online]. Available: -content/uploads/2020/04/SG-NTU-methanol-marine-report-Jan-2021-1.pdf.

[32] Svanberg M, Ellis J, Lundgren J, Landälv I. Renewable methanol as a fuel for the shipping industry. Renew Sustain Energy Rev 2018;94:1217–28. https://doi.org/10.1016/j.rser.2018.06.058.

[33] Corbett JJ, Winebrake JJ. Life cycle analysis of the use of methanol for Marin transportation. Prepared for US Department of Transportation Maritime Administration (MARAD). 2018.

[34] Harris K, Grim RG, Huang Z, Tao L. A comparative techno-economic analysis of renewable methanol synthesis from biomass and CO_2: opportunities and barriers to commercialization. Appl Energy 2021;303:117637. https://doi.org/10.1016/j.apenergy.2021.117637.

[35] Vogt KA, Vogt DJ, Patel-Weynand T, Upadhye R, Edlund D, Edmonds RL, et al. Bio-methanol: how energy choices in the western united states can help mitigate global climate change. Renewable Energy 2009;34(1):233–41.

[36] Baker SE, Stolaroff JK, Peridas G, Pang SH, Goldstein HM, Lucci FR, et al. Getting to neutral: options for negative carbon emissions in California. In: Lawrence Livermore National Laboratory Tech. Rep. LLNL-TR-796100; 2019. https://doi.org/10.2172/1597217.

[37] Taptich MN, Scown CD, Piscopo K, Horvath A. Drop-in biofuels offer strategies for meeting California's 2030 climate mandate. Environ Res Lett 2018;13(9). https://doi.org/10.1088/1748-9326/aadcb2. pp. 094 018.

[38] Tan ECD, Hawkins TR, Lee U, Tao L, Meyer PA, Wang M, et al. Biofuel options for marine applications: technoeconomic and life-cycle analyses. Environ Sci Technol 2021;55(11):7561–70. https://doi.org/10.1021/acs.est.0c06141.

[39] Hennig M, Haase M. Techno-economic analysis of hydrogen enhanced methanol to gasoline process from biomass-derived synthesis gas. Fuel Process Technol 2021;216:106776. https://doi.org/10.1016/j.fuproc.2021.106776.

[40] California Air Resources Board, *Low carbon fuel standard, basics*, Aug. 2021. [Online]. Available: https://ww2.arb.ca.gov/resources/documents/lcfs-basics.

[41] Jones A, Sherlock M, "The Tax Credit for Carbon Sequestration (Section 45Q)," *Congressional Re- search Service Report*, 2020.

[42] Port of Los Angeles, Port Of Los Angeles, Facts and Figures, Aug. 2021. [Online]. Available: https://kentico.portoflosangeles.org/getmedia/a8fcbf89-f5dd-4027-8ffc-cb743f478f87/2020-Facts-Figures.

[43] Methanol Institute, *Methanol: An Emerging Marine Fuel*, https://www.methanol.org/wp-content/uploads/2020/04/Methanol-Emerging-Marine-Fuel-Presentation.pdf/, Aug. 2020.

[44] Langholtz MH, Stokes BJ, Eaton LM, "2016 Billion-ton report: Advancing domestic resources for a thriving bioeconomy, Volume 1: Economic availability of feedstock," *Oak Ridge National Laboratory, Oak Ridge, Tennessee, managed by UT-Battelle, LLC for the US Department of Energy*, vol. 2016, pp. 1–411, 2016.

[45] Cabiyo B, Sanchez D, "Innovative Wood Use Can Enable Carbon Beneficial Forest Management in CA," 2019.

[46] Williams RB, Jenkins BM, Kaffka S, "An Assessment of Biomass Resources in California 2013", 2015.

[47] Mitchell KA, Parker NC, Sharma B, Kaffka S, "Draft Report: Potential for Biofuel Production from Forest Woody Biomass," 2015.

[48] Forest Climate Action Team, *California Forest Carbon Plan: Managing Our Forest Landscapes in a Changing Climate*, https://resources.ca.gov/CNRALegacyFiles/wp-content/uploads/2018/05/California-Forest-Carbon-Plan-Final-Draft-for-Public-Release-May-2018.pdf, 2018.

[49] CAL FIRE, *CAL FIRE Priority Projects 2019, Executive Order N-05-19*, Aug. 2021. [Online]. Available: https://calfire-forestry.maps.arcgis.com/apps/View/index.html?appid=749b9b262ed14622adbf07a5cb847d76.

[50] McIver CP, Meek JP, Scudder MG, Sorenson CB, Morgan TA, Christensen GA, "California's forest products industry and timber harvest, 2012," In *Gen. Tech. Rep. PNW-GTR-908. Portland, OR: US Department of Agriculture, Forest Service, Pacific Northwest Research Station. 49 p.*, vol. 908, 2015.

[51] White EM. Woody biomass for bioenergy and biofuels in the United States: A briefing paper. DIANE Publishing 2010;825.

[52] Wang M, Elgowainy A, Lee U, Bafana A, Benavides PT, Burnham A, Cai H, Dai Q, Gracida-Alvarez UR, Hawkins TR, et al. Summary of Expansions and Updates in GREET® 2020. Tech. Rep. Argonne, IL (United States): Argonne National Lab. (ANL); 2020.

[53] Sahoo K, Bilek ET, Mani S. Techno-economic and environmental assessments of storing woodchips and pellets for bioenergy applications. Renew Sustain Energy Rev 2018;98:27–39. https://doi.org/10.1016/j.rser.2018.08.055.

[54] Wright M, Brown RC. Establishing the optimal sizes of different kinds of biorefineries. Biofuels, Bioprod Biorefin: Innov Sustain Econ 2007;1(3):191–200.

[55] Scown CD, Baral NR, Yang M, Vora N, Huntington T. Technoeconomic analysis for biofuels and bioproducts. Curr Opin Biotechnol 2021;67:58–64. https://doi.org/10.1016/j.copbio.2021.01.002.

[56] Sahoo K, Bilek E, Bergman R, Mani S. Techno-economic analysis of producing solid biofuels and biochar from forest residues using portable systems. Appl Energy 2019;235:578–90. https://doi.org/10.1016/j.apenergy.2018.10.076.

[57] Satam CC, Daub M, Realff MJ. Techno-economic analysis of 1, 4-butanediol production by a single-step bioconversion process. Biofuels, Bioprod Biorefin 2019;13(5):1261–73. https://doi.org/10.1002/bbb.2016.

[58] Sun C, Theodoropoulos C, Scrutton NS. Techno-economic assessment of microbial limonene production. Bioresour Technol 2020;300:122666. https://doi.org/10.1016/j.biortech.2019.122666.

[59] Bates RB, Ghoniem AF. Biomass torrefaction: modeling of volatile and solid product evolution kinetics. Bioresour Technol 2012;124:460–9. https://doi.org/10.1016/j.biortech.2012.07.018.

[60] Bates RB, Ghoniem AF. Biomass torrefaction: Modeling of reaction thermochemistry. Bioresour Technol 2013;134:331–40. https://doi.org/10.1016/j.biortech.2013.01.158.

[61] Di Blasi C, Lanzetta M. Intrinsic kinetics of isothermal xylan degradation in inert atmosphere. J Anal Appl Pyrol 1997;40:287–303. https://doi.org/10.1016/S0165-2370(97) 00028-4.

[62] Nocquet T, Dupont C, Commandre J-M, Grateau M, Thiery S, Nguyen M, et al. Mass loss and gas release during torrefaction of biomass and its constituents. Ecole des mines d'Albi 2012.

[63] Prins MJ, Ptasinski KJ, Janssen FJ. Torrefaction of wood: Part 1. weight loss kinetics. J Anal Appl Pyrol 2006;77(1):28–34. https://doi.org/10.1016/j.jaap.2006.01.002.

[64] Prins MJ, Ptasinski KJ, Janssen FJ. Torrefaction of wood: Part 2. Analysis of products. J Anal Appl Pyrol 2006;77(1):35–40. https://doi.org/10.1016/j.jaap.2006.01.001.

[65] Nocquet T, "Torréfaction du bois et de ses constituants: Expériences et modélisation des rendements en matières volatiles," Ph.D. dissertation, 2012.

[66] Nocquet T, Dupont C, Commandre J-M, Grateau M, Thiery S, Salvador S. Volatile species release during torrefaction of biomass and its macromolecular constituents: part 2–modeling study. Energy 2014;72:188–94. https://doi.org/10.1016/j.energy.2014.05.023.

[67] Peduzzi E, Boissonnet G, Haarlemmer G, Dupont C, Maréchal F. Torrefaction modelling for lignocellulosic biomass conversion processes. Energy 2014;70:58–67. https://doi.org/10.1016/j.energy.2014.03.086.

[68] Van der Ploeg H, Chhoa T, Zuideveld P. The Shell coal gasification process for the US industry. Gasification Technol Conf 2004:1–19.

[69] Ferreira S, Monteiro E, Brito P, Vilarinho C. A holistic review on biomass gasification modified equilibrium models. Energies 2019;12(1):160. https://doi.org/10.3390/en12010160.

[70] Zainal Z, Ali R, Lean C, Seetharamu K. Prediction of performance of a downdraft gasifier using equilibrium modeling for different biomass materials. Energy Convers Manage 2001;42(12):1499–515. https://doi.org/10.1016/S0196-8904(00)00078-9.

[71] Prins MJ, "Thermodynamic analysis of biomass gasification and torrefaction.," 2005.

[72] McCoy ST, Rubin ES. An engineering-economic model of pipeline transport of CO_2 with application to carbon capture and storage. Int J Greenhouse Gas Control 2008;2(2):219–29. https://doi.org/10.1016/S1750-5836(07)00119-3.

[73] Grant T, Morgan D. FE/NETL CO_2 Transport cost model. Washington, DC: US Department Of Energy National Energy Technology Laboratory; 2018.

[74] Chang T, Rousseau RW, Kilpatrick PK. Methanol synthesis reactions: calculations of equilibrium conversions using equations of state. Ind Eng Chem Process Des Dev 1986;25(2):477–81. https://doi.org/10.1021/i200033a021.
[75] Graaf GH, Winkelman JG. Chemical equilibria in methanol synthesis including the water–gas shift reaction: a critical reassessment. Ind Eng Chem Res 2016;55(20): 5854–64. https://doi.org/10.1021/acs.iecr.6b00815.
[76] Turton R, Bailie RC, Whiting WB, Shaeiwitz JA. Analysis, synthesis and design of chemical processes. Pearson Education; 2008.
[77] Theis J, "Cost Estimation Methodology for NETL assessments of power plant performance," *US Department of Energy, National Energy Technology Laboratories, Report No. DOE/NETL-PUB-22580*, 2019.
[78] Nguyen T-V, Clausen LR. Techno-economic analysis of polygeneration systems based on catalytic hydropyrolysis for the production of bio-oil and fuels. Energy Convers Manage 2019;184:539–58. https://doi.org/10.1016/j.enconman.2019.01.070.
[79] Medina E, Wellon GC, Evegren F, *Methanol safe handling manual*, 2017.
[80] Stark AK. Multi-criteria lifecycle evaluation of transportation fuels derived from biomass gasification. Massachusetts Institute of Technology; 2010. Ph.D. dissertation.
[81] Rocha-Meneses L, Raud M, Orupõld K, Kikas T. Second-generation bioethanol production: a review of strategies for waste valorisation. Agronomy Res 2017;15 (3):830–47.
[82] Council NR, et al. Technologies and approaches to reducing the fuel consumption of medium-and heavy-duty vehicles. National Academies Press; 2010.
[83] Hank C, Gelpke S, Schnabl A, White RJ, Full J, Wiebe N, et al. Economics & carbon dioxide avoidance cost of methanol production based on renewable hydro- gen and recycled carbon dioxide–power-to-methanol. Sustainable Energy Fuels 2018;2(6): 1244–61. https://doi.org/10.1039/C8SE00032H.
[84] Carvalho L, Furusjö E, Kirtania K, Wetterlund E, Lundgren J, Anheden M, et al. Techno- economic assessment of catalytic gasification of biomass powders for methanol production. Bioresour Technol 2017;237:167–77. https://doi.org/10.1016/j.biortech.2017.02.019.
[85] Tan EC, Ruddy D, Nash CP, Dupuis DP, Dutta A, Hartley D, et al. High-octane gasoline from lignocellulosic biomass via syngas and methanol/dimethyl ether intermediates: 2018 state of technology and future research. Golden, CO (United States): National Renewable Energy Lab. (NREL); 2018. Tech. Rep.
[86] Bisson J, Han H-S. Quality of feedstock produced from sorted forest residues. Am J Biomass Bioenergy 2016;5:Jan. https://doi.org/10.7726/ajbb.2016.1007.
[87] Brandt KL, Gao J, Wang J, Wooley RJ, Wolcott M. Techno-economic analysis of forest residue conversion to sugar using three-stage milling as pretreatment. Front Energy Res 2018;6:77. https://doi.org/10.3389/fenrg.2018.00077.
[88] Kizha AR, Han H-S. Processing and sorting forest residues: cost, productivity and managerial impacts. Biomass Bioenergy 2016;93:97–106. https://doi.org/10.1016/j.biombioe.2016.06.021.
[89] Methanex, *Pricing*, https://www.methanex.com/our-business/pricing, Accessed: 2021-09-15, 2021.
[90] IEA, *Indicative shipping fuel cost ranges*, Aug. 2021. [Online]. Available: https://www.iea.org/data-and-statistics/charts/indicative-shipping-fuel-cost-ranges.
[91] Brynolf S, Fridell E, Andersson K. Environmental assessment of marine fuels: liquefied natural gas, liquefied biogas, methanol and bio-methanol. J Cleaner Prod 2014;74:86–95. https://doi.org/10.1016/j.jclepro.2014.03.052.
[92] Balcombe P, Brierley J, Lewis C, Skatvedt L, Speirs J, Hawkes A, et al. How to decarbonise international shipping: options for fuels, technologies and policies. Energy Convers Manage 2019;182:72–88.